Journal Name

ARTICLE TYPE

Cite this: DOI: 00.0000/xxxxxxxxxx

Techno-economic assessment of non-aqueous CO_2 reduction

Shashwati C. da Cunha[a] and Joaquin Resasco*[a]

Received Date
Accepted Date

DOI: 00.0000/xxxxxxxxxx

Most research on low-temperature CO_2 electrolysis has focused on aqueous electrolytes, primarily because non-aqueous systems require high cell voltages. However, CO_2R in aqueous electrolytes competes with hydrogen evolution and requires many electron transfers to produce C_{2+} molecules, challenges that can be suppressed in non-aqueous electrolytes. In this forward-looking techno-economic assessment, we model the product cost for non-aqueous CO_2R. We show that CO_2R to oxalic acid – a 2-electron C_2 product formed in non-aqueous electrolytes – is surprisingly affordable, although producing CO is more expensive in non-aqueous systems. Using parameters extracted from the largest collection of literature data on CO_2R in aprotic non-aqueous electrolytes, we find that oxalic acid would cost \$2.87/$kg_{oxalic\ acid}$ in a small-scale process. A commercial-scale plant would lower the product cost to \$1.56/$kg_{oxalic\ acid}$, approaching current market prices of \$0.7 to \$2.5/$kg_{oxalic\ acid}$. Capital cost for this process is dominated by product separation, while operating costs mostly arise from stack replacement and electricity to drive the high required cell voltage. This assessment shows that non-aqueous CO_2R could be a promising pathway for scale-up that has been largely overlooked compared to aqueous CO_2 electrolysis, offering new opportunities like electrolyte design to lower product costs. We therefore present a technical roadmap to make non-aqueous CO_2R to oxalic acid competitive with market prices.

0.1 Broader context

Electrochemical CO_2 reduction could utilize emitted CO_2 and surplus renewable electricity to manufacture chemicals with lower carbon footprints. In this study, we show that the emerging field of non-aqueous CO_2 reduction holds significant economic promise. Non-aqueous electrolytes often have low ionic conductivity, but allow for selective production of oxalic acid via just two electron transfers. Our techno-economic assessment and process model show that these differences make oxalic acid a more economical product than expected, although producing CO is expensive in non-aqueous environments.

C-C coupling to produce multi-carbon products is of special interest to unlock valuable chemical manufacturing routes from CO_2. Despite years of research in aqueous CO_2 electrolysis, making economical C_2 products remains challenging due to competing side reactions and the high number of electron transfers required to make these products. While aqueous C_2 products like ethylene have larger markets, the economics of CO_2R to oxalic acid could allow it to scale up efficiently, despite its early stage of technological development. Our physics-based techno-economic assessment therefore motivates further exploration of non-aqueous CO_2R to oxalic acid as an economical pathway for sustainable chemical manufacturing.

1 INTRODUCTION

Electrochemical CO_2 reduction (CO_2R) converts captured carbon dioxide into valuable chemical feedstocks and fuels using renewable electricity.[1] Water is typically used as both the reducing agent and solvent to convert CO_2 into various products, including carbon monoxide, formic acid, and ethylene. However, water can also be reduced to hydrogen on the electrode surface at operating voltages, limiting selectivity towards CO_2R. Since the main operating cost for CO_2R is the electric utility needed to drive electrolysis, current spent on the competing hydrogen evolution reaction (HER) can make the process prohibitively expensive.[2,3] To minimize water flooding and reduce cell resistance, zero-gap membrane electrode assembly (MEA) electrolyzers are used for scale-up, but most MEA designs lose selectivity with increasing single-pass conversions.[4] This is because CO_2 is quickly depleted by aqueous acid-base buffering reactions that convert it into (bi)carbonate anions.[5] The migration of these CO_3^{2-} ions carries away stoichiometric amounts of CO_2 from the surface. As a result, the maximum single-pass conversion is just 25% for many aqueous electrolyzers making ethylene. Overall, most studies agree that aqueous CO_2R is not commercially viable at current retail electricity prices, assuming a >50% reduction in electricity

[a] McKetta Department of Chemical Engineering, The University of Texas at Austin, Austin, TX 78712, USA. E-mail: resasco@utexas.edu

† Supplementary Information available. See DOI: 00.0000/00000000.

price to achieve economical CO_2R.[6–9]

CO_2R in non-aqueous solvents could circumvent several of these challenges. The HER is suppressed in aprotic solvents because of limited proton availability, improving selectivity towards CO_2R.[10] In the absence of protons, different membranes can also be chosen. Anion exchange membranes are often necessary in aqueous electrolytes to limit proton transport to the electrode surface, whereas proton exchange membranes (PEMs) like Nafion™ can be used in non-aqueous electrolytes without selectivity loss. PEMs are typically more conductive, mechanically stable, and chemically inert than anion exchange membranes.[11] These benefits have made Nafion™ a natural choice for membrane water electrolyzers despite the expensive IrO_x and RuO_x catalysts that are required to facilitate the anode reaction in acid.

Since PEMs preferentially conduct cations, they dramatically reduce the crossover of carbonate anions from cathode to anode.[12] Without carbonate crossover, non-aqueous systems could theoretically achieve high or complete single-pass conversion, and eliminate the need to recover CO_2 from the anode gas. This would lower the cost of separations and recycling.

Another potential advantage of non-aqueous CO_2R is the potential to generate alternative products that are not formed in aqueous conditions. In water, a series of proton-coupled electron transfer steps lead to the formation of hydrogenated products such as ethylene, ethanol, and methane. In contrast, aprotic environments enable the formation of oxalate through only two electron transfers without the involvement of protons.[13] The current requirement per mole of oxalate is six or more times lower than for aqueous C_{2+} products. On the other hand, CO and formate are formed in both aqueous and non-aqueous CO_2R via two electron transfers. Workbook S1 compares product properties for non-aqueous CO_2R.

Despite these benefits, non-aqueous CO_2R faces many technical challenges. Experimental demonstrations so far have been limited to low currents and short cell lifetimes. A series of works from Spurgeon and coworkers has attempted to change this, providing clarity on design principles for continuous non-aqueous CO_2R, but challenges remain with scale-up.[14–17] Although deionized water and common organic solvents have similarly low conductivities,[18] organic solvents cannot easily dissolve common supporting electrolytes like alkali metal halides and carbonates. To work around solubility constraints, expensive supporting electrolytes, such as ionic liquids or quarternary ammonium salts, are necessary. Even if supporting electrolytes are fully soluble, the relative permittivity of many organic solvents is lower than that of water, limiting ion pair dissociation.[19] Despite these technical challenges, mature electrochemical technologies, including various battery chemistries, rely on non-aqueous electrolytes with large electrochemical windows, high thermal stability, and adequate conductivity.[20] Although these electrolytes can be expensive and challenging to synthesize, they are designed to resist degradation and evaporation, reducing the amount of electrolyte needed over the lifetime of a system. While some electrolyte design principles may be transferable, ohmic losses in flow cells can be more dramatic because of larger electrolyte chambers and higher current density.

Recent advances in understanding and designing non-aqueous electrolytes for CO_2R[21,22] have renewed interest in the field. Although cell voltages in aprotic solvents are typically higher than in aqueous cells, previous work[8,23] has shown that high selectivity, especially on a molar basis, can offset other disadvantages. A physics-informed techno-economic assessment (TEA) is necessary to quantify the impacts of these performance tradeoffs, like increased resistance and alternate reaction pathways, on process costs. Given recent developments in non-aqueous electrolysis,[21,24,25] a complete TEA of non-aqueous CO_2R is timely.

Additionally, prior TEAs evaluating the commercial potential of aqueous CO_2R show that these processes, especially to ethylene, usually require large reductions in the cost of electricity to be economical.[6,7,9] Other C_{2+} products from aqueous CO_2R are likely to be even more expensive since their typical selectivity is even lower than that of ethylene.[2,26] While these chemicals have some of the largest global manufacturing volumes,[27] alternative CO_2R products that can compete with current market prices would be easier to scale, playing their own role in industrial decarbonization.

In this work, we therefore perform a detailed TEA of non-aqueous CO_2R, and appeal to the field to consider how its development can be accelerated. TEAs on specific or simplified non-aqueous CO_2R technologies have found some promise, especially for producing oxalic acid.[7,28,29] We similarly find that CO_2R to oxalic acid may be a promising pathway, and go on to identify opportunities to lower product costs. We also assess the possible impact of unique research opportunities in non-aqueous electrolyzers, such as electrolyte design.

1.1 Approach

1.1.1 CO_2R products in aprotic electrolytes

In this study, we evaluate the techno-economics of oxalic acid and CO produced through non-aqueous CO_2R. Oxalate is most commonly produced over Pb catalysts in aprotic electrolytes[13] and forms oxalic acid through protonation by trace water that crosses the PEM. Its market price in North America averages \$0.7/kg, but prices in Europe are as high as \$2.5/kg.[30] It is used in the pharmaceutical and textile sectors for synthesis, in fiber processing for textiles, and as a rust remover.[31] The global market for these applications is estimated at \$0.9 – \$1.1 billion,[32,33] and is expected to grow to \$1.5 – \$2.3 billion by 2033.[34] Additional applications are being explored, especially in polymer synthesis.[35] The global production of oxalic acid is over 3,300 t/day and projected to grow to 5,000 t/day.[30]

In addition to oxalic acid, non-aqueous CO_2R can selectively produce CO over various noble metal catalysts in aprotic electrolytes, including Ag and Cu.[36] CO is a versatile feedstock with existing pathways for conversion into fuels, fibers, and resins.[1] Formic acid can be made selectively under certain non-aqueous conditions,[10] but they tend to be highly specific. In aqueous conditions, CO and formic acid can both be produced selectively, while a distribution of C_{2+} products is typically formed over Cu catalysts.[37] Reaction schema for this work can be found in the Methods section (4.2).

To contextualize process costs, we compare our techno-economics with market prices and aqueous CO_2R for each product. Given the small process scales assessed in this work, direct comparisons to market price are misleading. We therefore compare aqueous and non-aqueous pathways for CO_2R to CO at the same scale. Since there is no aqueous pathway to oxalic acid, we provide process costs alongside the most economical aqueous C_2 product, ethylene. Although ethylene has a much larger market, the similar product prices between these C_2 products give context to the advantages and disadvantages of the oxalic acid pathway, without being dominated by process scale effects. Assessing the viability of aqueous CO_2R pathways is beyond the scope of this work – for example, aqueous C_{2+} products could leverage unique process integrations, which have been discussed at length elsewhere.[38–40]

1.1.2 Process design and techno-economic assessment

We consider a process design involving a CO_2 electrolyzer, downstream product separations, and recycle streams for electrolytes and unreacted CO_2. Operational challenges unique to non-aqueous CO_2R, such as solvent loss and water crossover, are taken into account in the process design. Gas mixtures are separated by pressure swing adsorption (PSA).[41] We assume oxalic acid is extracted by gas-antisolvent precipitation (GASP).[42,43] Capital costs are based on unit sizes derived by mass balance. Although alternative cathodes like Pb are cheaper than the precious metals used in aqueous CO_2R, electrolyzer capital cost is dominated by the cost of iridium at the anode.[44,45] We therefore assume that aqueous and non-aqueous CO_2 electrolyzers have the same capital cost.[45]

Feedstock needs are derived by mass balance, and utility costs from the energy consumption for each unit. Most other operating overheads are proportional to the total capital cost. When comparing aqueous and non-aqueous CO_2R, we use identical market assumptions (including United States average retail electricity costs, product prices, feedstock costs) and process scale (production in t/day throughout this work). We make several highly conservative assumptions for the non-aqueous process, including a high HER selectivity, the catholyte exiting the electrolyzer with 20% water, and annual stack replacement over a short 10-year plant lifetime. On the other hand, we assume that operating current densities will exceed today's state of the art to reach a base case of 200 mA/cm^2.

2 RESULTS AND DISCUSSION

2.1 State-of-the-art in benchtop non-aqueous CO_2R

To establish a base case for our TEA, we first conducted a literature review of non-aqueous CO_2R in aprotic solvents. Figure 1 summarizes the performance of a number of state-of-the-art aprotic CO_2 electrolyzers. This collection, expanded from the work of Dos Reis et al.,[46] is the largest compiled dataset on aprotic non-aqueous CO_2R literature to our knowledge. It covers different scales, reactor designs, and electrolytes, but excludes non-aqueous protic solvents, notably ethanol and methanol. This is because the CO_2R mechanism and product distribution differ in aprotic versus protic solvents.[13]

Systematic comparison of the non-aqueous CO_2R literature is challenging due to the wide range of operating conditions used. For example, studies use different solvents, supporting electrolytes, reactor configurations, water concentrations, and reference electrodes. Consequently, Figures 1a – f do not reveal clear trends between variables. Furthermore, it is clear that state-of-the-art performance in non-aqueous CO_2R lags behind aqueous CO_2R, especially in terms of current density and stability testing. The operating duration of CO_2R in non-aqueous solvents is orders of magnitude below commercial requirements ($>$10,000 hours).[44] This is partly because long-term tests are rarely attempted. We account for these short experiment durations by assuming that stack lifetime for non-aqueous CO_2 electrolyzers is 5 times shorter than aqueous. A more precise estimate is challenging because failure modes are rarely reported, although flooding of gas diffusion electrodes and salt precipitation have been observed in both both aqueous and non-aqueous electrolyzers.[25,47]

The raw data (Workbook S2) can also be categorized by electrolyte (Figure S1, ESI†), again revealing an absence of clear trends. Segregating the data by reactor type shows that high currents have only been achieved in two reactor designs: undivided cells with sacrificial metal anodes, and flow cells with gas diffusion electrodes (Figure S2, ESI†). The highest stable current density achieved in an aprotic electrolyte, to our knowledge, is 80 mA/cm^2.[24,48] Typical applied potentials are -2 to -4 V at total current densities $\geq$ 15 mA/cm^2, depending on the catalyst, solvent and supporting electrolyte.

Based on these observations and process considerations, we performed our TEA assuming a flow electrolyzer design with gas diffusion electrodes. Oxalic acid, oxalate ions, and metal oxalates are formed via the same cathode reaction. Although undivided cells have been used to produce metal oxalates, these products lack industrial applications today. Metal oxalates could be processed, for example via ion exchange, to make oxalic acid indirectly. Since this TEA does not include downstream upgrading, we limit our analysis to oxalic acid and CO.[48]

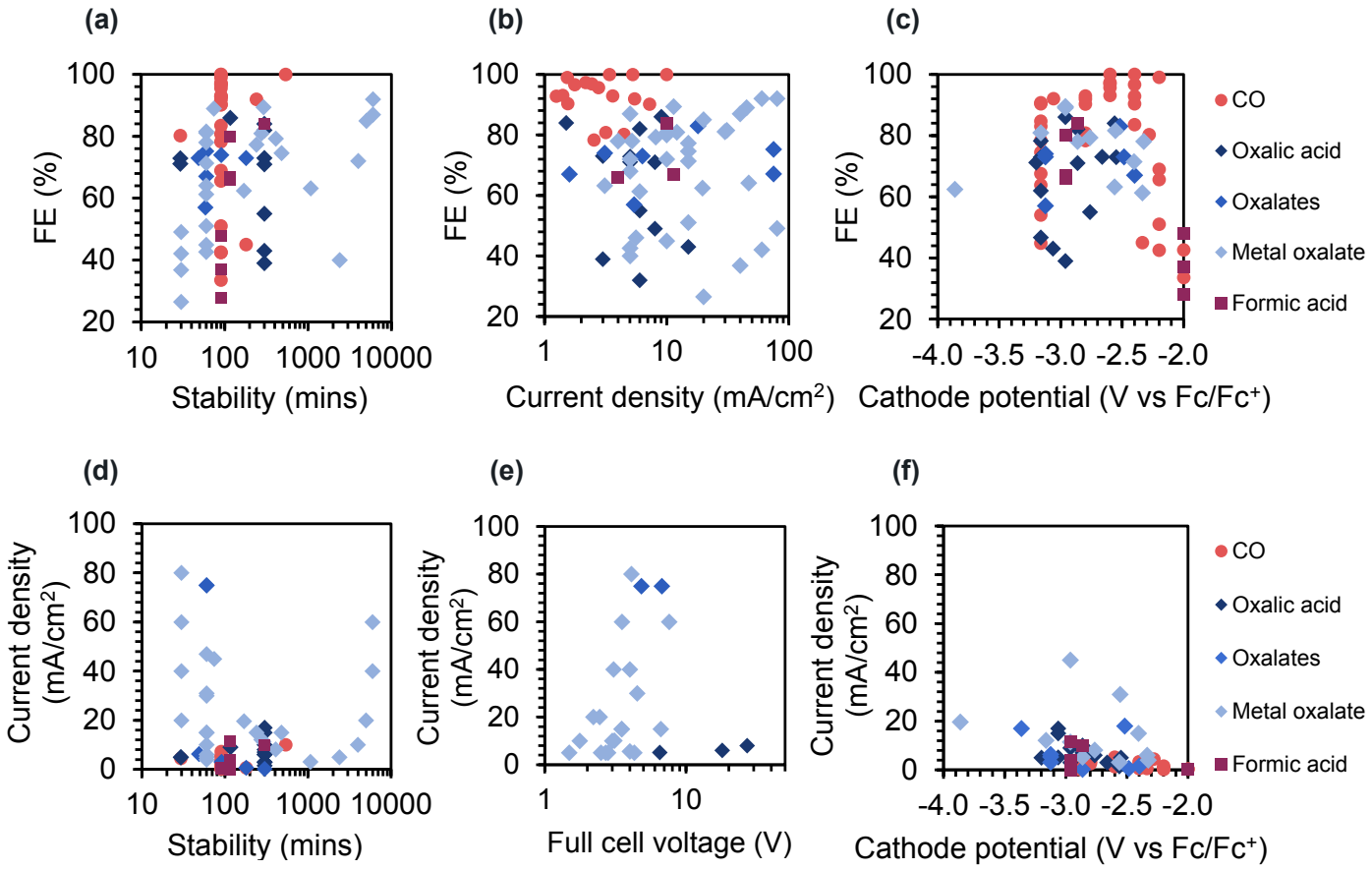

Fig. 1 Performance reported for bench-scale non-aqueous CO_2R does not show clear trends. Each marker type represents a product. Workbook S2 and Figure S1 (ESI†) list all source data. (a) Selectivity to the main CO_2R product versus stability. (b) Selectivity versus total current density. (c) Selectivity versus applied cathode potential. (d) Total current density versus stability. (e) Total current density versus full-cell voltage, where reported. Few studies report full-cell voltages. (f) Total current density versus applied cathode potential.

2.2 Comparing aqueous and non-aqueous CO_2R processes

Given that non-aqueous CO_2R is a new technology, we elected to model a relatively small process scale of 3 $t_{product}$/day for this TEA. Below this production rate, the effects of economy of scale outweigh any changes in performance. A larger scale would represent a very large facility for a new oxalic acid process, given that a large operating commercial plant makes 71 $t_{oxalic\ acid}$/day.[49] However, 3 t/day is much smaller than a commercial scale plant for CO or ethylene (30 – 2000 t/day).[50,51] Critically, CO_2R is not expected to be cost-competitive at such a small scale, especially for CO and ethylene, since commodity market prices benefit from existing economies of scale in larger plants. To account for this effect of production rate, we compare the costs of non-aqueous CO_2R against an aqueous CO_2R process of the same scale.

We assume that aqueous CO_2R will use the best-case electrolyzer design from our recent TEA,[8] namely a membrane electrode assembly design that is able to decouple selectivity from single-pass conversion. This could be accomplished through flow field re-design, a subject of ongoing research.[52] We optimized current density and single-pass conversion for this scenario. The optimal cell voltage for the aqueous MEA making CO is 2.92 V at a total current density of 464.5 mA/cm^2, with an optimal selectivity of 88% at 46.7% single-pass conversion. For the aqueous MEA making ethylene, the optimal cell voltage is 3.25 V at 428.3 mA/cm^2 and the optimal selectivity is 70% at 18.9% single-pass conversion. Key base-case parameters for the aqueous and non-aqueous processes can be found in Table 1, with complete lists in Table S3 (ESI†) and Workbook S1.

2.2.1 Electrolyzer design for non-aqueous CO_2R

We base our TEA on incumbent technologies as much as possible. The non-aqueous electrolyzer is assumed to be a flow cell with gas diffusion electrodes in an aprotic/protic configuration (Figure S2b, ESI†). This design couples a non-aqueous catholyte with an aqueous anolyte, separated by a PEM. At the cathode, we assume that CO_2R takes place at a metal-coated gas diffusion electrode, with one side contacting CO_2 and the other an aprotic non-aqueous solvent containing 0.3 M of supporting electrolyte.[24] Both aqueous and non-aqueous CO_2R at the cathode are paired with aqueous oxygen evolution at the anode, allowing the direct use of well-developed catalysts from water electrolysis. Aqueous CO_2R is assumed to occur in a neutral electrolyte, making the cathode surface alkaline.

We model cell voltage as a combination of thermodynamic potentials of CO_2R and oxygen evolution, their kinetic overpotentials from the Butler-Volmer equation, and ohmic losses due to membrane and catholyte resistance (Figures S3c and d, ESI†).[8] The ohmic resistance of aprotic electrolytes is orders of magnitude higher than that of the anion exchange membranes used for aqueous CO_2R. In our analysis, we compare four common aprotic solvents – acetonitrile (ACN), dimethyl sulfoxide (DMSO), propylene carbonate (PC), and 1,2-dimethylformamide (DMF). In the main text, we report results for the solvent that yields the lowest levelized product cost (DMF for CO, DMSO for oxalic acid). We also focus on a representative non-aqueous supporting electrolyte, tetraethylammonium chloride (TEACl), which offers higher conductivity than salts with larger, less mobile ions. CO_2R kinetics are modeled using a representative exchange current density and Tafel slope. For simplicity, we assume that these values vary little with solvent, as observed previously.[22] In reality, kinetic parameters are unique for a combination of catalyst, solvent, and electrolyte. Solvents can also affect selectivity, especially in the presence of water.[21] To account for unique electrolytes that could therefore have complex effects, we test thousands of theoretical combinations of electrolyte-dependent parameters via a Monte Carlo simulation.

Given the short durations of non-aqueous experiments today, we assume that the non-aqueous plant operates for 10 years with a stack lifetime of 1 year, whereas the aqueous CO_2R process operates for 20 years with a stack lifetime of 5 years. We also assume a binary product distribution where only H_2 is generated as a byproduct.

2.2.2 Process design differences for non-aqueous CO_2R

Figure 2 compares the process design for aqueous CO_2R generating gas-phase products (Figure 2a) with non-aqueous CO_2R generating gas-phase products (Figure 2b) or liquid-phase products (Figure 2c). Figure 2a shows CO as a product, but the process is identical for ethylene production, since we assume a binary product distribution.[8] Stream numbers are consistent between Figures 2a – c, so some are non-sequential. Apart from differences in the separation units, the volatile catholyte may need to be replenished by a make-up (Stream 18) in case of electrolyte evaporation, electrolysis, thermal degradation, separation losses, or contamination (represented as a purge, Stream 21). Since the aprotic catholyte (Stream 19) and aqueous anolyte (Stream 4) are separated by a water-permeable membrane, water will cross the membrane from the anode to cathode side. The catholyte must be dried to maintain steady-state moisture levels.

To separate CO_2 from gas-phase CO and H_2, pressure-swing adsorption (PSA) is used in all three cases. Aqueous CO_2R also requires a PSA unit to separate O_2 from the CO_2 that crosses the membrane as CO_3^{2-}. In non-aqueous CO_2R, Nafion™ limits anion transport, so there is no need for CO_2 recovery from the anode gas. Oxalic acid is a liquid product, so Figure 2c includes gas separation only for CO_2/H_2. Separating liquid products from the non-aqueous solvent is expensive and difficult, particularly because the supporting electrolyte must remain in the solvent phase. Unlike CO and ethylene, which spontaneously phase-separate into the gas stream, oxalic acid is highly soluble in non-aqueous solvents.[53–55] Its low sublimation point also limits the use of thermal methods.[56] The only reported method to directly separate oxalic acid from an aprotic solvent in CO_2R is gas-antisolvent precipitation (GASP), where CO_2 is dissolved into the mixture at supercritical pressures to crash out oxalic acid.[28,57,58] Chemical methods, like the reaction of acidic oxalic acid with metal ions and re-constitution after liquid-liquid extraction, have also been proposed.[48] Here, we use GASP to estimate base case costs. Given its low technology readiness level, we also report sensitivity to changing the capital cost and efficiency of oxalic acid separation.

Drying the catholyte is typically a challenge when operating non-aqueous CO_2R. Many lab-scale experiments maintain

Table 1 Key parameters and results for the four CO_2R base cases compared. Sources are listed in Table S3 (ESI†) and Workbook S1.

Parameter	Unit	CO, aqueous MEA	Ethylene, aqueous MEA	CO, DMF/TEACl	Oxalic acid, DMSO/TEACl	Notes
Production rate	$t_{product}$/day			3		
CO_2 cost	$/$t_{CO2}$			75		Point source CO_2 capture, mid-range
Electricity cost	$/kWh			0.082		U.S. industrial retail average, 2024
Electrolyzer capital cost	$/m^2			5174		Iridium anode
Total current density	mA/cm^2	465	428	200	200	Optimized for minimum cost in aqueous cases; optimistic for non-aqueous
Cell voltage	V	2.92	3.25	5.05	5.98	Modeled polarization curve
Ohmic loss	V	0.46	0.43	1.2	2.0	Modeled polarization curve
Stack area	m^2	58.7	478.3	134.4	53.2	Mass balance and current density
Faradaic efficiency		0.88	0.70	0.89	0.70	Literature
Single-pass conversion		0.467	0.189	0.667	0.667	Optimized for minimum cost in aqueous cases with stoichiometric crossover; optimistic for non-aqueous
Plant lifetime	years	20	20	10	10	
Stack lifetime	years	5	5	1	1	
Market price	$/kg	0.85	0.96	0.85	0.70	Literature
Capital cost, 3 t/day	million $	3.06	11.91	4.10	5.61	Total permanent investment
Operating cost, 3 t/day	$/kg	2.02	7.54	3.16	2.34	
Levelized cost, 3 t/day	$/kg	2.17	8.10	3.55	2.87	

<1 ppm water content, and avoid hygroscopic supporting electrolytes.[21] At higher water levels, selectivity towards the hydrogen evolution reaction dominates over CO_2R.[10] But recent studies have shown that some wet solvents – including upto 3 M H_2O – can still give high CO_2R selectivity, and also lower cell voltages.[21,59,60] Our chosen base case solvents, DMF and DMSO, are water-tolerant according to these emerging electrolyte design principles.[21]

To counteract water transport to the cathode by electro-osmotic drag,[11] the non-aqueous CO_2R process (Figures 2b, c) has a liquid drier unit on Stream 24. While drying is time-consuming in the lab, many industrial processes maintain streams as dry as -40 °C dew point. This is commonly achieved using multiple drying stages that finish with dessicant drying (for instance, over molecular sieves or alumina). We assume that large water quantities are removed by cheap and simple filtration and/or knockout units. Trace water is removed using an MS4A dessicant bed consisting of two parallel units that are periodically regenerated by purging with an inert gas. We assume there is chemical compatibility between the solvent, supporting electrolyte, and dessicant, since all three are quite inert at ambient temperature. We neglect the small quantity of water that could hydrate oxalate, which is slightly hygroscopic and often exists as a crystalline dihydrate ($(COOH)_2 \cdot 2H_2O$).[61]

In all cases, the capital costs of pumping and compression are lumped into the balance-of-plant, since they are small compared to reaction and separation units. We estimate that pumping and compression account for <2% of process energy requirement despite the viscosity increase for non-aqueous electrolytes, so we neglect their energy demand. Similarly, we neglect the relatively small cost of anolyte purification by ion exchange.[8]

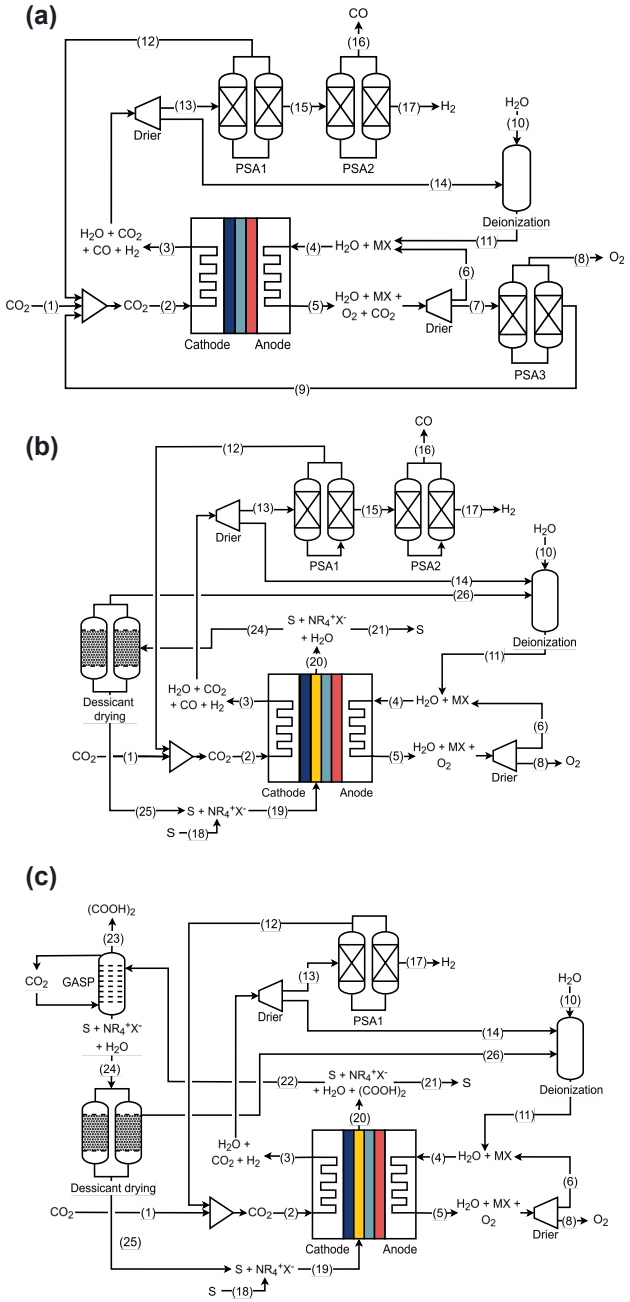

Fig. 2 Process flow diagrams for aqueous and non-aqueous CO_2R. (a) Process flow diagram for CO_2R to CO in an aqueous MEA with electrolyte MX.[8] The process design is identical for CO_2R to ethylene, since we neglect selectivity to other products. (b, c) Process flow diagram for non-aqueous CO_2R to (b) CO and (c) oxalic acid. Non-aqueous CO_2R in (b) and (c) occurs in solvent S with supporting electrolyte $NR_4^+X^-$, coupled with the oxidation of water to oxygen.

2.3 The economics of scaling up non-aqueous CO_2R

2.3.1 Capital cost

Figures 3 and 4 examine the capital expenditures (capex) of non-aqueous CO_2R. Figures 3a and 3b compare the capital costs for a CO_2R process using an aqueous MEA versus a non-aqueous flow cell. To account for the effect of economy of scale on prices, we contextualize process costs for non-aqueous CO_2R with aqueous CO_2R at the same mass flow rate of product. Figure 3a breaks down the capex for aqueous and non-aqueous CO_2R producing 3,000 kg_{CO}/day. Figure 3b compares the process capex for an aqueous MEA making 3,000 $kg_{ethylene}$/day to a non-aqueous flow cell producing 3,000 $kg_{oxalic\ acid}$/day. Trends in the costs of these four pathways are similar at other process scales, and for an analysis performed at a fixed carbon utilization rate. Ethylene is provided solely as a reference C_2 product with a similar unit price to oxalic acid. Given the much larger typical process scale for ethylene, whose market is 200 – 300 times larger than that of oxalic acid,[62] this assessment cannot be directly used to interpret the costs of CO_2R to ethylene.

For CO production (Figure 3a), the capex is similar in aqueous and non-aqueous systems ($3.1 – 4.1 million). However, producing oxalic acid in non-aqueous electrolyte (Figure 3b) requires less than half of the capex ($5.6 million) of producing ethylene in aqueous conditions ($11.9 million). The main driver of capex is the cost of separation units in all cases. The capital costs of the non-aqueous solvent and supporting electrolyte are small compared to the electrolyzer and separation units.

The electrolyzer cost for CO_2R to CO is nearly double in the non-aqueous system than the aqueous ($0.78 million versus $0.34 million) (Figure 3a). This is because of the lower total current density for operation. Resistive aprotic electrolytes lead to high cell voltages which reduce the optimal current density to 300 – 400 mA/cm^2 (Figure S3, ESI†), compared to 465 mA/cm^2 in the aqueous MEA. Based on literature performance (Figure 1), we assume that state-of-the-art non-aqueous CO_2R will operate at only 200 mA/cm^2 at the base case. Since both processes make the same amount of CO, the electrolyzer area is higher for the non-aqueous case, which increases the electrolyzer cost linearly.

Since there is no carbonate crossover in non-aqueous CO_2R, we assume that a higher single-pass conversion is accessible (66.7% conversion to CO in DMF compared to 46.7% in the MEA), while selectivities are similar (89% and 88% for CO_2R to CO). This reduces the total stream size of recycled CO_2. However, the resulting reduction in unit sizes for gas separation for non-aqueous CO_2R is outweighed by the additional material cost for stainless steel units to tolerate the acidic conditions. For non-aqueous CO_2R to CO, capex savings from eliminating the CO_2/O_2 PSA3 unit are more than compensated by the larger electrolyzer and stainless steel units. The liquid drying unit is an additional capital cost as well. Overall, the total permanent investment to produce 3,000 kg_{CO}/day is slightly lower in aqueous ($3.06 million) than non-aqueous electrolyte ($4.10 million).

The differences are more pronounced for C_2 products (Figure 3b). Oxalic acid (90 g/mol) is much heavier than ethylene (28 g/mol), so producing 3,000 $kg_{oxalic\ acid}$/day requires a process that is over three times smaller. Additionally, the single-pass conversion to ethylene is optimal at just 18.9%, compared to 66.7% assumed here for oxalic acid. This is because the single-pass conversion of CO_2 to ethylene is severely limited by the 12 electron transfers required per product molecule, which causes high carbonate crossover.[5] Gas separation costs are therefore much larger when producing ethylene than oxalic acid or CO. The GASP liquid-liquid separation to extract oxalic acid from the catholyte requires a high enough volumetric flow rate of CO_2 to reach supercriticality,[43] above which oxalic acid is presumed to precipitate selectively. The unit size and capex of liquid-liquid separation thus scale with the flow rate of CO_2 required. DMSO, which has the lowest CO_2 solubility of the solvents assessed here, therefore yields the lowest costs for CO_2R to oxalic acid.

CO_2R to ethylene requires 12 electron transfers per molecule, resulting in a 6× higher partial current per mole than CO_2R to oxalate. We assume that the MEA operates at its optimal current density of 428 mA/cm^2, whereas the non-aqueous flow cell operates at only 200 mA/cm^2 (compared to its optimal current density of 309 mA/cm^2). Despite the higher current density, the electrolyzer size for the ethylene process is about 9× larger (costing $2.77 million for ethylene vs $0.31 million for oxalic acid). This is a result of the 3.2× higher molar flow rate of product, 6× higher current per mole of product, and 2× higher total current density. Realistic selectivities will likely widen this difference in electrolyzer cost. While we generously assume nearly identical selectivities of 70% for CO_2R to ethylene and oxalic acid, ethylene is rarely reported at such high selectivity and is typically accompanied by a range of byproducts. However, there are many reports that meet or exceed this selectivity for oxalic acid, including with only H_2 as a byproduct. Despite the additional cost of liquid/liquid separation and the optimistic assumptions made for CO_2R to ethylene, the total permanent investment to produce 3,000 $kg_{oxalic\ acid}$/day in a non-aqueous process is $5.61 million, less than half of an aqueous analog producing 3,000 $kg_{ethylene}$/day ($11.91 million).

Figures 4a and 4b show the uni-variate sensitivity of the total permanent investment in non-aqueous CO_2R towards electrolyzer and process parameters from design and operation. Without optimizing current density, the capital cost is insensitive to cell voltage (and any parameters that contribute only to cell voltage, like catalyst kinetics and resistance). Capex increases with the amount of non-aqueous electrolyte required, especially the expensive supporting electrolyte. It therefore increases with catholyte flow rate (represented by the excess solvent ratio, i.e. the ratio between molar flow rate of solvent and CO_2 fed to the cathode). Increasing current density reduces the required electrolyzer area and lowers capital cost. Lower single-pass conversion increases capex due to larger stream volumes. Lower selectivity and higher production rates both increase the process size, increasing capex. For oxalic acid production, increasing CO_2 solubility increases the amount of CO_2 required for GASP, driving up capex.

Figures 4c and 4d show the uni-variate sensitivity of the total permanent investment in non-aqueous CO_2R to market variables. The additional capital cost of common aprotic solvents is negligi-

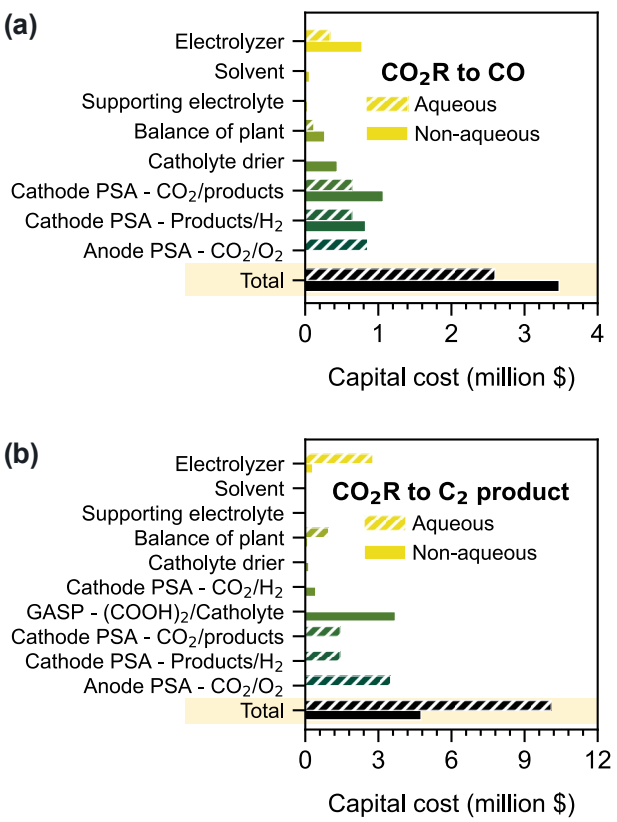

Fig. 3 Capital costs for small-scale aqueous and non-aqueous CO_2R processes making 3 $t_{product}$/day. (a, b) Bare-module capex breakdown for aqueous and non-aqueous CO_2R to (a) CO and (b) C_2 products (ethylene and oxalic acid). Aqueous CO_2R occurs in an MEA, non-aqueous CO_2R to CO in DMF/TEACl, and non-aqueous CO_2R to oxalic acid in DMSO/TEACl.

ble. The supporting electrolyte contributes exclusively to capital cost since it is completely recycled due to its electrochemical stability and low volatility. Expensive supporting electrolytes, like novel ionic liquids that must be synthesized in small batches, can considerably increase cost. We assume a low base case cost of \$10/kg of supporting electrolyte, which has been quoted for quaternary ammonium salts that are already used in some industrial processes.[63] As expected from the above discussion, electrolyzer and separation unit costs strongly affect the total permanent investment. In particular, capex is highly sensitive to the cost of gas and liquid separations; assessing further advancements in separation technologies is beyond the scope of this work.

2.3.2 Operating cost

Figure 5 breaks down the operating expenditure (opex) and levelized cost for aqueous and non-aqueous CO_2R processes making 3,000 kg/day of product. The operating cost on a mass basis is lower for aqueous than non-aqueous CO_2R to CO (\$2.02/kg_{CO} compared to \$3.16/kg_{CO}). However, the opex for non-aqueous CO_2R to oxalic acid (\$2.34/$kg_{oxalic\ acid}$) is less than a third of the opex for aqueous CO_2R to ethylene (\$7.54/$kg_{ethylene}$) – note the small process scale, which contributes to the high ethylene price. In all scenarios, utility costs – primarily electricity for electrolysis (Figures S4 and S5, ESI†) – are a major operating expense (Figures 5a and 5b). Non-aqueous CO_2 electrolyzers have especially high utility costs due to their high cell voltages (5.05 V for CO, 5.98 V for oxalic acid at 200 mA/cm^2 in our flow cell model), compared to about 3 V in the aqueous MEAs around 450 mA/cm^2. The high opex of ethylene production is largely driven by the 12 electron transfers required per molecule of product, which leads to a high total current, increasing the required electric utility.

In Figure S3 (ESI†), we show the polarization curve and sensitivity of cost to lower current density operation in non-aqueous CO_2R. The calculated ohmic drops (1.22 V for CO and 2.0 V for oxalic acid) are well within the electrochemical window of the solvent (Table S2, ESI†), avoiding the risk of solvent decomposition. Supporting electrolytes also have a window of electrochemical stability (about 6 V for the tetraalkylammonium salts listed here)[64] and must tolerate the ohmic drop associated with high current operation. Additionally, our solvent conductivities may be slightly underestimated compared to the literature.

We assume that non-aqueous CO_2R will be able to operate at 200 mA/cm^2 in an aprotic/protic flow cell, although current densities >80 mA/cm^2 have only been shown in undivided cells with sacrificial anodes. Recent work from Spurgeon and coworkers has demonstrated similar current densities when cycling methanol/water flow cells, and discussed pathways for further improvements.[65] Even if current density cannot be increased, the levelized cost varies by <10% over a large range of current densities. For non-aqueous CO_2R to oxalic acid, halving the total current density from 200 mA/cm^2 to 100 mA/cm^2 increases the levelized cost by just 9%, from \$2.87/$kg_{oxalic\ acid}$ to \$3.14/$kg_{oxalic\ acid}$ (Figure S3, ESI†). Operating significantly above the optimal current density is economically disadvantageous, since increased ohmic drop outweighs the benefit of a smaller electrolyzer unit (Figure S3, ESI†).[8]

Most other operating expenses are similar for aqueous and non-aqueous CO_2R. The overall process size for 3,000 kg_{CO}/day is much larger than 3,000 $kg_{oxalic\ acid}$/day, since the molar mass of CO is lower so the total current is much higher. The electrolyzer cost is therefore higher for CO_2R to CO than to oxalic acid, as is the catholyte stream size that needs to be dried. Stack and dessicant replacement costs scale directly with the process size, so they significantly differ between CO and oxalic acid. For non-aqueous CO_2R to CO, the large and frequent cost of stack replacement is significant, contributing to the high opex for non-aqueous CO_2R to CO (\$3.16/kg_{CO}) compared to aqueous (\$2.02/kg_{CO}). Utility savings lead to a low opex for non-aqueous CO_2R to oxalic acid (\$2.34/$kg_{oxalic\ acid}$) compared to aqueous CO_2R to ethylene (\$7.54/$kg_{ethylene}$).

2.3.3 Levelized cost

Figures 5c and 5d break down the levelized cost of producing CO and oxalic acid from CO_2R at 3 $t_{product}$/day. Given the lower electrolyzer and utility cost, CO_2R to CO is 40% cheaper in aqueous (\$2.17/kg_{CO}) than non-aqueous electrolytes (\$3.55/kg_{CO}). However, the lower current requirement drives savings of 65% in the levelized cost of non-aqueous CO_2R to oxalic acid (\$2.87/$kg_{oxalic\ acid}$) compared to aqueous CO_2R to ethy-

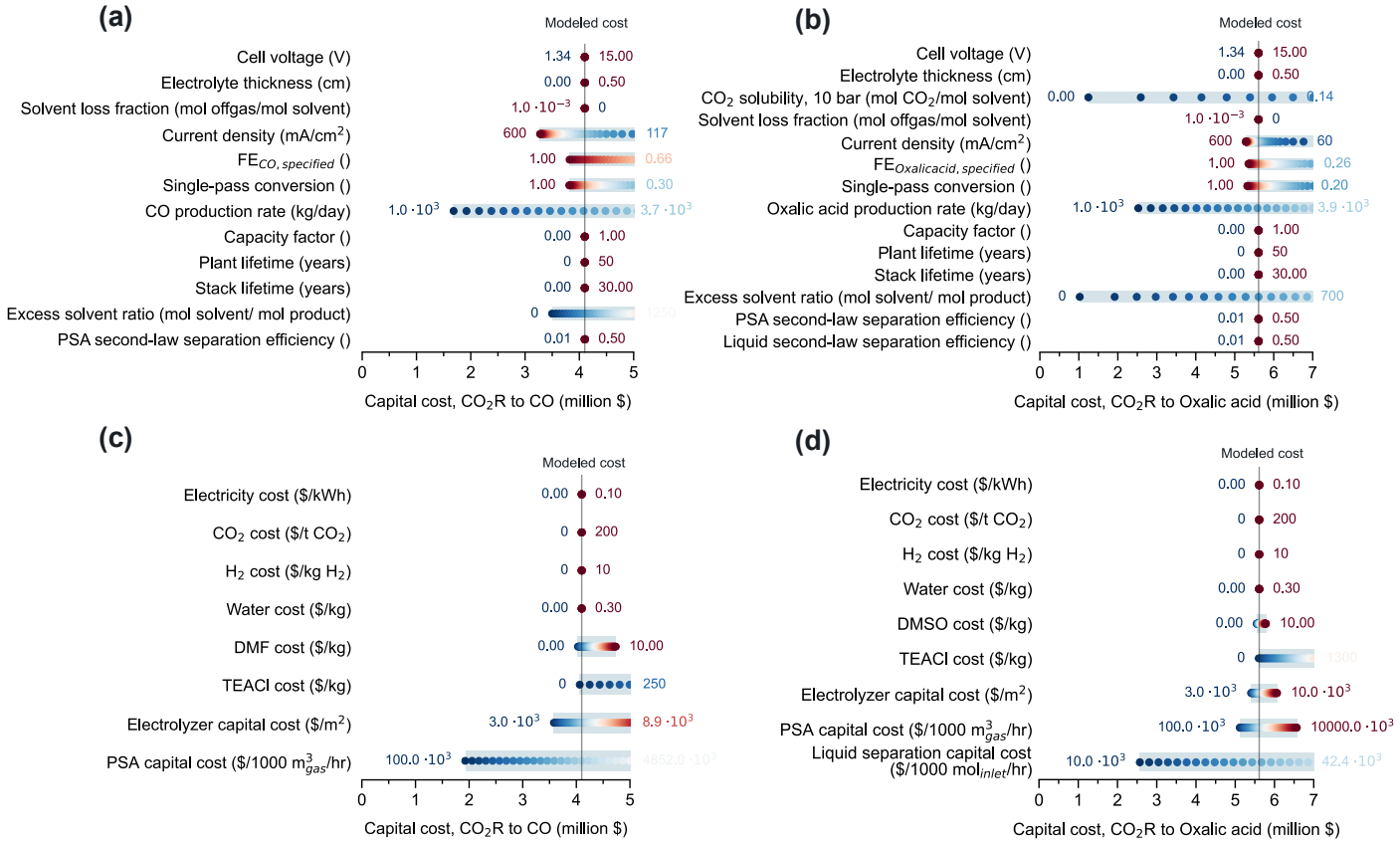

Fig. 4 Univariate sensitivity of capital costs for small-scale aqueous and non-aqueous CO_2R processes making 3 $t_{product}$/day. (a, b) Sensitivity of total permanent investment to process and electrolyzer parameters for non-aqueous CO_2R to (a) CO and (b) oxalic acid. (c, d) Sensitivity of total permanent investment to market parameters for non-aqueous CO_2R to (c) CO and (d) oxalic acid. Non-aqueous CO_2R to CO occurs in DMF/TEACl, and non-aqueous CO_2R to oxalic acid in DMSO/TEACl.

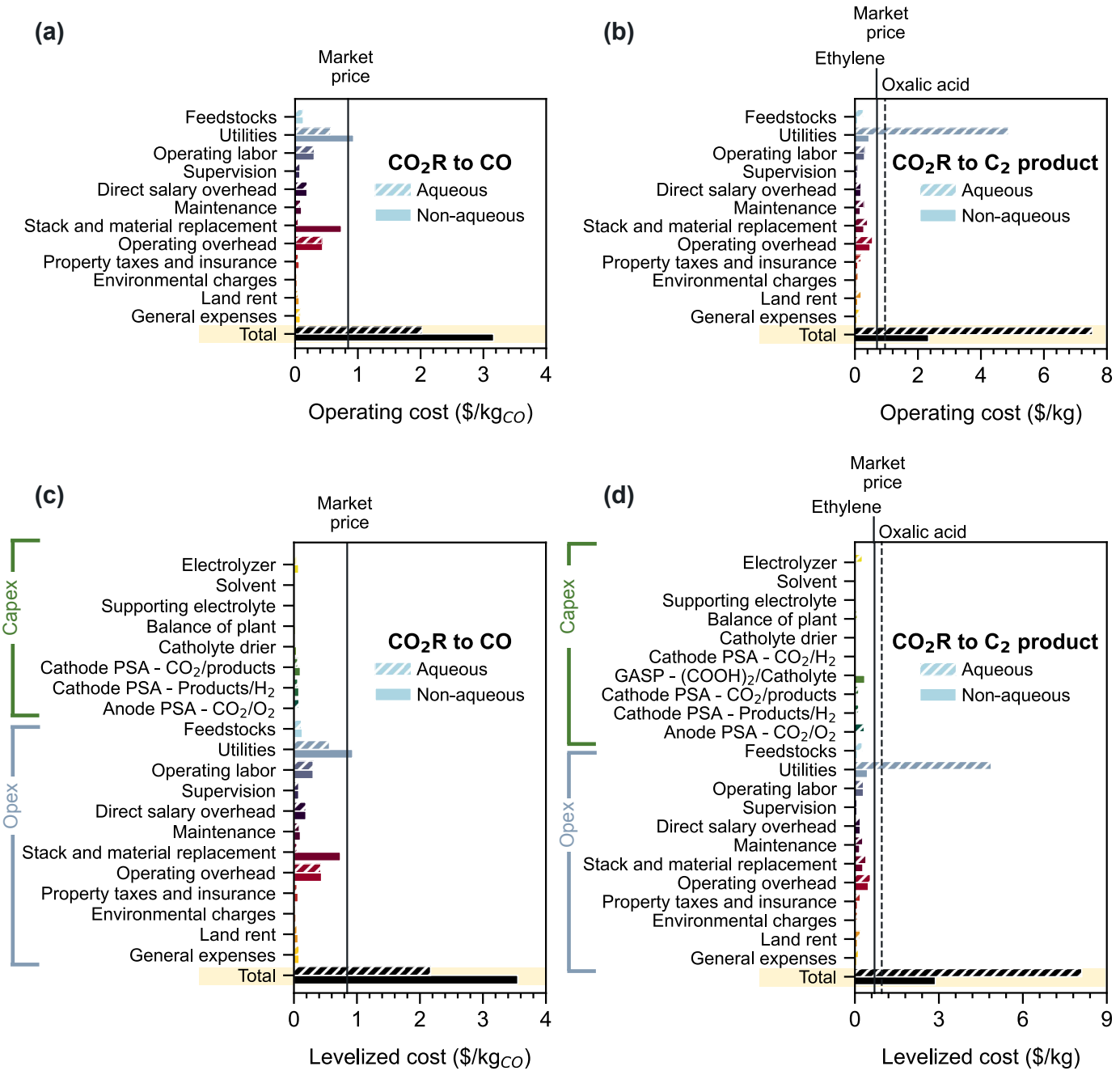

Fig. 5 Operating and levelized costs for small-scale aqueous and non-aqueous CO_2R processes making 3 $t_{product}$/day. (a, b) Opex breakdown for aqueous and non-aqueous CO_2R to (a) CO and (b) C_2 products (ethylene and oxalic acid). (c, d) Levelized cost breakdown for aqueous and non-aqueous CO_2R to (c) CO and (d) C_2 products. Aqueous CO_2R occurs in an MEA, non-aqueous CO_2R to CO in DMF/TEACl, and non-aqueous CO_2R to oxalic acid in DMSO/TEACl.

lene ($8.10/$kg_{ethylene}$). This difference is a result of both capex and opex being significantly lower for oxalic acid production than ethylene. Net present value and breakeven cost for the non-aqueous processes can be found in Figures S6 and S7 (ESI†). Although these results compare levelized costs on a mass basis at 3 $t_{product}$/day, the relative economic viability of non-aqueous CO_2R is the same on a mass basis at 30 $t_{product}$/day, and when comparing the levelized cost of carbon utilization for 30 $t_{CO2\ utilized}$/day.

At this scale, none of the four evaluated processes are commercially viable due to insufficient economies of scale. Although capex is a small fraction of the levelized cost in all scenarios, many components of the opex scale proportionally with capex on an annualized basis (for example, maintenance is 4% of the plant cost per year). Compared to large-scale analyses,[8,38,66] this contribution of capex-dependent costs is magnified at the small process scale modeled here. Utilities, especially electricity for electrolysis, contribute more significantly to the levelized cost at commercial process scales (Figure S8, ESI†).

Figure 6 shows the sensitivity of the levelized cost of non-aqueous CO_2R towards various process and operational parameters (Figures 6a and b) and market variables (Figures 6c and d). The effects of economy of scale are clear in the large improvement in levelized cost at higher production rates. Since utility costs are a major component of the opex, the levelized cost of producing both CO (Figure 6a) and oxalic acid (Figure 6b) is highly sensitive to cell voltage. Separations need a small fraction of the process energy compared to electrolysis, so improvements in separation efficiency have a smaller effect on levelized cost than cell voltage. Other critical factors influencing costs include selectivity, single-pass conversion, stack lifetime, and the amount of solvent required. On the market side, the prices of electricity, supporting electrolyte, and separation units dramatically affect levelized cost. The levelized cost of CO is more sensitive to these parameters than oxalic acid because of the larger plant size required.

We can further break down the sensitivity towards cell voltage into its components. Electrolyte resistance is a major contributor to cell voltage and therefore to energy demands for non-aqueous CO_2R. Improving electrolyte conductivity would therefore improve the economics of non-aqueous CO_2R. Ohmic resistance could also be reduced by shortening the length of the catholyte chamber between the cathode and the membrane. These developments, which lower cell voltage, would reduce the opex. Stable operation at the optimal current density, which is higher than the base case, would reduce the levelized cost by balancing capex and opex tradeoffs.[8] Regarding reaction kinetics, the Tafel slope of non-aqueous CO_2R is in the range of 100-200 mV/dec, which is somewhat higher than aqueous CO_2R. The main kinetic limitation in our model is the slow exchange current density for non-aqueous CO_2R at the base case. This explains why levelized cost is highly sensitive to cathode overpotential, but not cathode Tafel slope. In fact, the ohmic resistance of non-aqueous electrolyte and slow cathode kinetics are the main reason why CO production is more economical in the aqueous MEA than non-aqueous flow cell. The anode catalyst (IrO_x) and membrane (Nafion™) are highly optimized, leaving little room for additional improvements in anodic overpotential or membrane conductivity.

Electrolyte costs are much higher for non-aqueous CO_2R than aqueous. Expensive supporting electrolytes contribute to capex-dependent opex, which is a conceptual representation of stricter process conditions, more complex maintenance, and so on. Organic solvents are expensive, volatile, and pose toxicity concerns, requiring special handling to minimize offgassing (e.g. pressurization with inerts). Degradation may also occur, especially given the high cell voltages and extended operation. We assume a solvent loss rate of 10^{-5} mol/s offgas or degradation per mol/s solvent fed, corresponding to a liquid flow rate of 1.7 L_{DMF}/hr for CO and 0.5 L_{DMSO}/hr for oxalic acid at 3,000 kg/day. At this rate, the entire solvent volume would need replacement over 4.1 years (63.4 m^3 for CO; 17.9 m^3 for oxalic acid). Higher solvent losses have major impacts on the process economics because of the cost of solvent replacement.[27]

Improving selectivity and single-pass conversion significantly reduces levelized cost. In aqueous systems, single-pass conversion is limited to 50% for CO and 25% for ethylene because of carbonate crossover. Most MEA designs today cannot even approach this limit due to effective plug flow behavior,[4] but our comparisons assume that they will overcome this design issue to reach the limit imposed by crossover.[8] We assume the non-aqueous electrolyzer operates at 66.7% conversion at the base case, which leaves little room for improvement through single-pass conversion alone. As expected, longer plant lifetimes, stack lifetimes, or higher capacity factors improve economics, since they provide more operational time for the same investment.

Figures 6c and 6d illustrate the sensitivity of the levelized cost of non-aqueous CO_2R towards market variables. Electricity cost has a large impact because utilities contribute so much to the opex. Electricity prices, especially from renewables, have declined steadily in recent years, although transmission and distribution costs have increased in the United States. This trend is likely to make electrochemical processes more economically attractive in the near future. Another major economic impact comes from the cost of the supporting electrolyte. Even though the supporting electrolyte is purchased only twice over 10 years, the cost of synthesizing a more complex electrolyte at scale could be prohibitive. Changes to electrolyzer and separations capex also make a large impact, especially at this small process size (Figure S8, ESI†). In summary, the levelized cost of non-aqueous CO_2R is highly sensitive to process scale, cathode overpotential, stack lifetime, electricity cost, supporting electrolyte cost, and process unit capex. The sensitivity of opex alone towards these variables can be found in Figure S9 (ESI†).

2.4 Pathways to economical CO_2R to oxalic acid

2.4.1 Electrolyte engineering effects

A unique feature of non-aqueous CO_2R is the vast electrolyte design space. The possible combinations of ionic supporting electrolytes are too numerous to test.[67] Cations may include alkylammoniums, imidazoliums, phosphoniums and pyrrolidiniums. Anions, including halides, fluoroborates, and so on, have a less direct effect on CO_2R performance,[22] but influence conductivity, costs, synthetic pathways, and more. There are strict require-

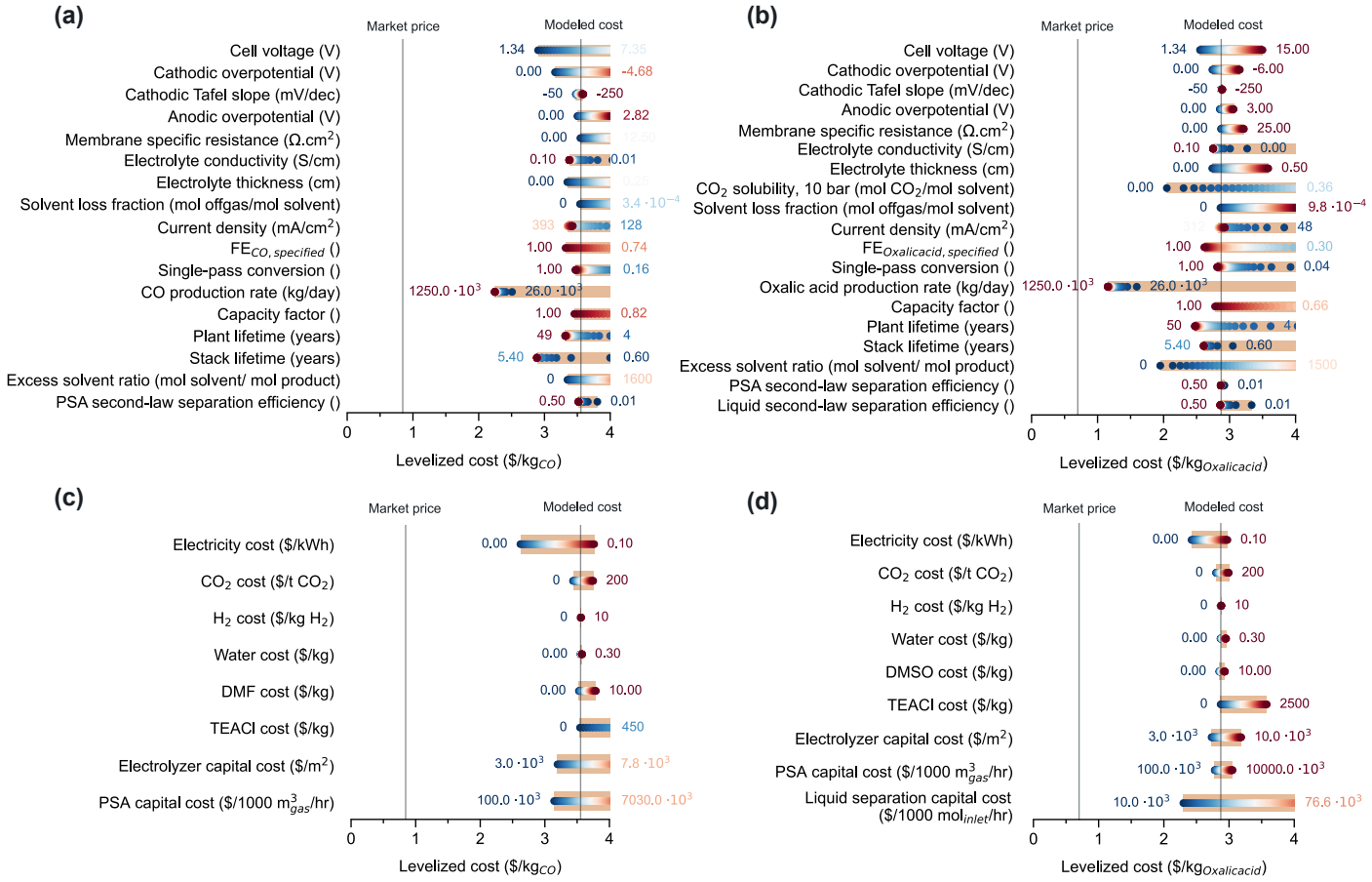

Fig. 6 Sensitivity of levelized cost of non-aqueous CO_2R. (a, b) Sensitivity to process and electrolyzer parameters for non-aqueous CO_2R to (a) CO and (b) oxalic acid. (c, d) Sensitivity to market parameters for non-aqueous CO_2R to (c) CO and (d) oxalic acid. Non-aqueous CO_2R to CO occurs in DMF/TEACl, and non-aqueous CO_2R to oxalic acid in DMSO/TEACl.

ments for the electrolyte: it must be electrochemically stable, inert towards reactants, products, and catalysts, highly conductive, and form a fully dissolved phase. These properties may be independent or correlated depending on the electrolyte design. They can depend on fundamental properties of both the solvent and supporting electrolyte, such as their dielectric constant, relative permittitivity, Lewis basicity, viscosity, effective ion diameter, and ionic strength.[21,68] While battery research provides some guidance for non-aqueous electrolyte design, major mechanistic, operational, and design differences limit direct translation.

To give a sense of how electrolyte design could influence costs of a full-scale production plant in the future, we conducted a Monte Carlo assessment at a 30 $t_{product}$/day scale. The TEA model was run 5,000 times to represent possible electrolytes, randomly sampling electrolyte-dependent properties, such as ionic conductivity, selectivity, and solvent cost. Figure 7 shows the resulting distribution of costs for random theoretical electrolytes. The sampled variables are the costs of solvent and supporting electrolyte, cathode overpotential, electrolyte conductivity, current density, selectivity, and solvent loss fraction (representing volatility or stability). The variables and their ranges, which vary from well below to well above their values at the base case, are listed in Table S6 (ESI†). For oxalic acid, there are three additional variables that arise from liquid-liquid separation: separation efficiency, unit capex, and CO_2 solubility. The capital cost of liquid-liquid separation of oxalic acid could introduce large uncertainties to costs, which is noteworthy given the novelty of GASP. Electrolyte design can be optimized to allow product separation via more mature methods like solvent-solvent extraction or oxalic acid crystallization.

Both capex and opex show a wide distribution depending on electrolyte properties, as seen in Figure 7. For comparison, the base case levelized cost at 30 $t_{product}$/day is \$2.48/kg_{CO} and \$1.56/$kg_{oxalic\ acid}$. The difference between this base case and the peaks in Figures 7c and 7f indicates that electrolyte design could reduce costs. Cost breakdowns for the base case in other solvents are shown in Figures S10, S11, S12, and S13 (ESI†). It is unlikely that electrolyte engineering alone will make non-aqueous CO_2R profitable. Comprehensive research at all scales remains essential for non-aqueous CO_2 electrolyzers.

2.4.2 Roadmap for further cost improvements

In Figure 8, we outline a pathway to economical production of oxalic acid by non-aqueous CO_2R (at \$0.63/$kg_{oxalic\ acid}$). The largest cost improvement comes from scaling up the process from 3 $t_{oxalic\ acid}$/day to 30 $t_{oxalic\ acid}$/day, which alone would lower the levelized product cost from \$2.87/$kg_{oxalic\ acid}$ to \$1.56/$kg_{oxalic\ acid}$. Other substantial improvements come from reducing the amount of solvent required for the process, increasing the current density, and reducing the electrolyte thickness. The electricity cost in this work is considerably higher than most TEAs and strongly influences product costs. For example, at \$0.05/kWh, the price of ethylene in a 30 t/day process also drops to \$4.84/kg (Figure S14, ESI†). Lower electricity prices are included in this roadmap based on progress in generation technologies. For instance, the cost of onshore wind generation coupled

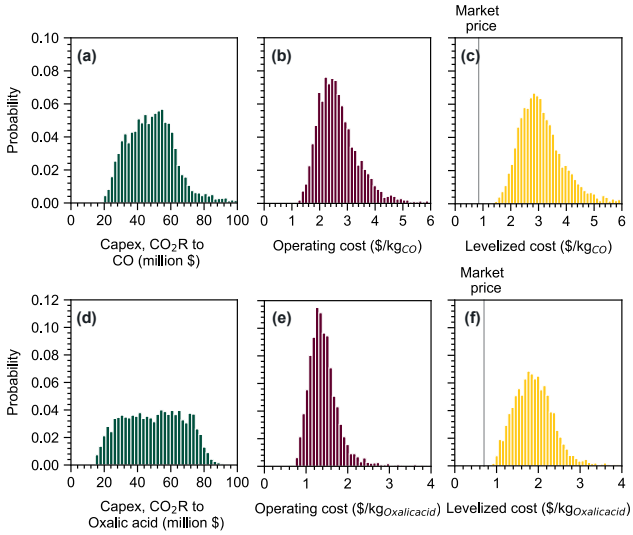

Fig. 7 Distributions of cost for non-aqueous CO_2R over randomly sampled electrolyte properties at 30 $t_{product}$/day. (a, d) Distributions of capex for non-aqueous CO_2R to (a) CO and (d) oxalic acid. (b, e) Distributions of opex for non-aqueous CO_2R to (b) CO and (e) oxalic acid. (c, f) Distributions of levelized cost for non-aqueous CO_2R to (c) CO and (f) oxalic acid.

to utility-scale storage is as low as \$0.042/kWh before transmission and distribution.[69] Significant savings could also result from reducing the cost of liquid/liquid separation, either by decreasing the capital cost of separation, or by reducing the CO_2 flow rate required for GASP. The latter option is not listed in Figure 8 because of the complex consequences of modifying CO_2 solubility.

3 CONCLUSIONS

In this work, we examine the techno-economic viability of low-temperature CO_2 reduction in non-aqueous electrolytes. Although C_{2+} molecules have great promise to expand synthetic pathways from CO_2, aqueous C_2 products remain expensive due to their low selectivity and high current requirements. We show that non-aqueous CO_2R to oxalic acid would cost \$2.87/$kg_{oxalic\ acid}$ in a 3 t/day plant with a capital cost of \$5.6 million, making it a cost-effective C_2 product. Moreover, we outline a roadmap to bring it below market price (to \$0.63/$kg_{oxalic\ acid}$). Oxalic acid has many existing and possible applications, including upgrading into oxalate- and glycolate-based polymers. Given the limited efforts in scaling up CO_2R to oxalic acid, especially compared to ethylene, it presents a timely and promising opportunity.

The immediate priority for a proof-of-concept of CO_2R to oxalic acid is demonstrating stable, selective operation at total current densities of 100 – 200 mA/cm^2. Our results are based on a 1 year stack lifetime and current densities $\geq$100 mA/cm^2. Beyond this, the top research priority should be lower cell voltage. Both catalyst and electrolyte development for non-aqueous field CO_2R are limited, leaving scope for progress. Cell voltage could be lowered directly by improving electrolyte conductivity, but an easier option may be to design microfluidic cells or microchanneled catholyte flow fields, which have been demonstrated in aqueous

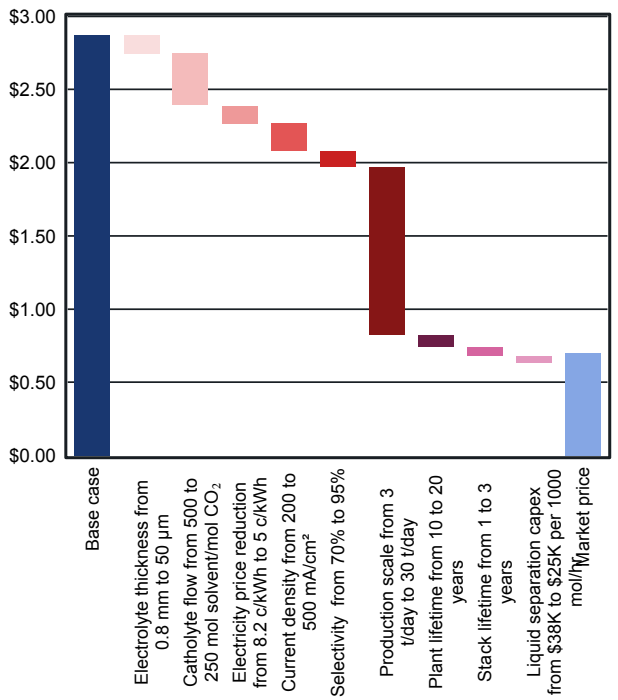

Fig. 8 Pathway to cost-competitive non-aqueous CO_2R to oxalic acid. Unless specified, other parameters remain at their base case values for CO_2R in DMSO/TEACl.

GDEs and fuel cells.[70,71] Improving the kinetics of non-aqueous CO_2R, guided by mechanistic understanding, would also be beneficial. The mechanism for CO_2 electrolysis into oxalate has been under debate for decades.[72,73] Unlike products with multiple adsorbed intermediates, like ethylene, it is theoretically possible to design an optimal catalyst for CO_2R to oxalate without being limited by scaling relationships.[74] We also need investigations of catholyte stability, including side reactions at the anode that could interfere with OER. These may impact electrolyte make-up costs, environmental concerns, downstream separations, and so on.

We also identify parameters that have minimal impact on the viability of non-aqueous CO_2R. Increased CO_2 solubility, frequently emphasized since it increases the kinetic current density of CO_2R, is less important at high currents ($\geq$ 100 mA/cm^2) that tend to be mass transfer limited. To operate at such high reaction rates, flow cells or MEAs in both aqueous and non-aqueous electrolytes will likely need gas diffusion electrodes that are limited by CO_2 diffusion rather than dissolution. In the case of oxalic acid, the use of supercritical CO_2 as an antisolvent for separation actually encourages the use of an electrolyte with low CO_2 solubility. Finally, typical solvent viscosities ($\leq$ 5 cP) are insignificant at the process scale, since the energy demand for pumping is negligible compared to electrolysis. On the microscopic scale, high viscosity can limit solution conductivity, indirectly impacting cell voltage.

Some parameters may prove to be important but are beyond the scope of the current TEA. Material compatibility is far less established for non-aqueous solvents than aqueous. While these electrolytes are fairly inert, it is critical that all parts of the process equipment can withstand them over long timescales. The toxicity of solvents explored here ranges from problematic to hazardous, compared to relatively safe aqueous brines. Also, directly integrating carbon capture and conversion may be possible in some non-aqueous systems. However, assessing the resulting trade-offs, like those in aqueous bicarbonate electrolyzers, is beyond the scope of this work. Lastly, cathode overpotential is a complex function of catalyst, supporting electrolyte, and solvent, which we simplified by screening a range of electrolyte properties through a Monte Carlo simulation. Further experimental studies, especially evaluations of multiple operating conditions and materials in the same electrolyzer, are necessary to further update the techno-economics of non-aqueous CO_2R.

4 EXPERIMENTAL PROCEDURES

4.0.1 Data and code availability

- The dataset analyzed in Figure 1 is available as an Excel workbook (.xlsx) in this paper's supplemental information.

- The original code for techno-economic assessment is available as a folder (.zip) in this paper's supplemental information.

4.1 Computational methodology

The electrolyzer model, process model, and economic calculations for non-aqueous CO_2R are calculated in Jupyter notebooks written in Python, using parameters imported from an Excel workbook. Each datapoint in this work, such as a point on the sensitivity analyses in Figure 6, is generated by a single run of the model. In each run, the cell voltage is calculated first, followed by stream and energy tables, and then capital and operating costs for the complete process. The cost of aqueous CO_2R is modeled using the method discussed in our prior work, which is very similar to the non-aqueous case described below.[8]

4.2 Electrolyzer model

We assume that the following chemical reactions can occur in the aprotic non-aqueous CO_2R environment:

Cathode reactions:

$$2CO_2 + 2e^- \rightarrow CO + CO_3^{2-} \tag{1}$$

$$CO_3^{2-} + 2H^+ \text{ (trace)} \rightleftharpoons CO_2 + H_2O \text{ (trace)} \tag{2}$$

$$2CO_2 + 2e^- \rightarrow ({}^-CO_2)_2 \tag{3}$$

$$({}^-CO_2)_2 + 2H^+ \text{ (trace)} \rightarrow (COOH)_2 \tag{4}$$

$$2H^+ \text{ (trace)} + 2e^- \rightarrow H_2 \tag{5}$$

Anode reaction:

$$H_2O \rightarrow 2H^+ + 2e^- + \frac{1}{2}O_2 \tag{6}$$

Net cell reactions:

$$CO_2 \rightarrow CO + \frac{1}{2}O_2 \tag{7}$$

$$2CO_2 + H_2O \rightarrow (COOH)_2 + \frac{1}{2}O_2 \tag{8}$$

We assume that the following chemical reactions can occur in the aqueous CO_2R environment:

Cathode reactions:

$$CO_2 + H_2O + 2e^- \rightarrow CO + 2OH^- \tag{9}$$

$$2CO_2 + 8H_2O + 12e^- \rightarrow C_2H_4 + 12OH^- \tag{10}$$

$$2H_2O + 2e^- \rightarrow H_2 + 2OH^- \tag{11}$$

Anode reaction:

$$2OH^- \rightarrow \frac{1}{2}O_2 + H_2O + 2e^- \tag{12}$$

Carbonate equilibrium:

$$CO_2 + 2OH^- \rightleftharpoons HCO_3^- + OH^- \rightleftharpoons CO_3^{2-} + H_2O \tag{13}$$

The single-pass conversion and Faradaic efficiency for non-aqueous CO_2R are specified as parameters from Workbook S1. We assume a binary product distribution. Therefore, all current goes towards forming either the target product or hydrogen, respectively with Faradaic efficiencies of FE_{H_2} and FE_{CO_2R}:

$$FE_{H_2} = 1 - FE_{CO_2R} \tag{14}$$

In the case of the aqueous MEA used for comparison, we assume that the selectivity FE_{CO_2R} is a weak function of the single-pass conversion X_{CO_2}, as modeled by Kas et al.[75] This is described in detail in our prior work.[8] Briefly, we fit the following functional form to the data collected by Kas et al. for FE_{H_2} versus X_{CO_2}:

$$FE_{H_2} - 3.93\% = 4.7306 \cdot {X_{CO_2}}^{5.4936} \tag{15}$$

$$\implies FE_{CO} = 96.07\% - 4.7306 \cdot {X_{CO_2}}^{5.4936} \tag{16}$$

We generalize this equation by assuming that 96.07% in the above equation corresponds to the maximum achievable selectivity as $X_{CO_2} \rightarrow 0$, a parameter called $FE_{CO_2R,0}$. We assume that the fitted parameters 4.7306 and 5.4936 are independent of the product. Therefore, the equation used to determine selectivity as a function of single-pass conversion in the aqueous cases is:

$$FE_{CO_2R} = FE_{CO_2R,0} - 4.7306 \cdot {X_{CO_2}}^{5.4936} \tag{17}$$

The process size is measured through a production rate in $kg_{product}$/day. We use Faraday's law to interconvert between currents and molar flow rates:

$$i_{CO_2R} = n_i \cdot F \cdot \dot{N}_{CO_2R\,product} \tag{18}$$

$$i_{total} = \frac{i_{CO_2R}}{FE_{CO_2R}} \tag{19}$$

$$i_{H_2} = i_{total} - i_{CO_2R} \tag{20}$$

$$i_{O_2} = i_{total} \tag{21}$$

where i_{total} is the total current to all products, i_{CO_2R} is the current towards CO_2R, n_i is the number of electrons transferred per mole of product, F is Faraday's constant, $\dot{N}_{CO_2R\,product}$ is the mole flow rate of product, and i_k is the current towards each product k. From Equations 14 and 18, all partial and total current densities are known for a given product mass flow rate. These currents are absolute values, which simplifies the calculation of the overpotential at each electrode.

The total current density i_{total} is used to calculate the active electrode area A based on the total current density j_{total}, which is a parameter:

$$A = \frac{i_{total}}{j_{total}} \tag{22}$$

$$j_i = \frac{i_i}{A} \tag{23}$$

We do not need to directly account for this area being divided into a stack, since the electrolyzer cost scales linearly with total active area. The current density towards each redox reaction comes from dividing their respective partial currents i_k by the electrolyzer area A.

We model the electrolyzer unit as a flow cell (Figure S2b, ESI†). The voltage drop across the cell therefore consists of the cathode potential ($E^0_{CO_2R} + \eta_{CO_2R}$), ohmic drop over the membrane and the catholyte (E_Ω), and anode potential ($E^0_{OER} + \eta_{OER}$). The equilibrium cell voltage $E^0_{cell} = E^0_{CO_2R} - E^0_{OER}$ is based on standard reduction potentials, uncorrected for experimental conditions by the Nernst equation.[76] The overpotentials at the cathode and anode are calculated using a Tafel relationship to achieve the specified partial current density towards CO_2R and OER, respectively. Ohmic losses are calculated from Ohm's law for the membrane and the electrolyte. Estimated cell potentials (5 – 6 V at 200 mA/cm^2) are comparable to other works (see Workbook S2).

$$E_{cell} = E^0_{CO_2R} - E^0_{OER} + \eta_{CO_2R} - \eta_{OER} + E_\Omega \tag{24}$$

$$\eta_i = \eta_{i,ref} + TS_i \cdot \log_{10}\left(\frac{j_i}{j_{i,ref}}\right) \tag{25}$$

$$E_\Omega = -i_{total} \cdot \Omega_{cell} \tag{26}$$

where E^0_i is the equilibrium potential for reaction i, η_i is the overpotential associated with the reaction i occuring at an electrode, $\eta_{i,ref}$ is a reference overpotential, TS_i is the Tafel slope, j_i is the reference current density, Ω is the cell resistance (in Ω). This simplified electrolyzer model ignores concentration polarization, HER current, and mass transport throughout.

Here, the cell resistance Ω comes from both the membrane and catholyte resistance:

$$\Omega_{cell} = \Omega_{membrane} + \Omega_{catholyte} \tag{27}$$

$$\Omega_{membrane} = \frac{\Omega'}{A} \tag{28}$$

$$\Omega_{catholyte} = \frac{1}{\kappa} \cdot \frac{l_{catholyte}}{A} \tag{29}$$

where $\Omega_{membane}$ is the resistance of the membrane, $\Omega_{catholyte}$ is the resistance of the catholyte, Ω' is the area-specific resistance of the membrane (in $\Omega{\cdot}cm^2$), κ is the ionic conductivity of the electrolyte in S/cm, and $l_{catholyte}$ is the catholyte chamber thickness. In the aqueous CO_2R models above, there is no catholyte since the cell design is assumed to be an aqueous MEA. Therefore, $\Omega = \Omega_{membrane}$ in the aqueous cases.

4.3 Mass and energy balances

4.3.1 Mole balances

Steady-state mass balances are calculated starting from the production basis, $\dot{N}_{CO_2R\,product}$, which corresponds to the molar flow rate of Stream 16 for CO ($\dot{N}_{\text{product (16)}}$) or of Stream 23 for oxalic acid ($\dot{N}_{\text{product (23}}$) in the process flow diagrams (Figure 2). Unit sizes, stream properties, and utilities are based on this mass balance. All stream numbers are referenced from Figure 2; we duplicate stream numbers between the three PFDs for clarity. (To maintain this consistency, some stream numbers are missing in each of the three PFDs; for example, the CO cases lack Stream 23 since there is no liquid product, whereas the oxalic acid case lacks Stream 16 since there is no gas CO_2R product.) Stream compositions in the electrolyzer are determined based on parameters like single-pass conversion and selectivity. We assume that all separations are perfect (100% selective). For quick reference, Table S1 (ESI†) includes stream numbers and their descriptions. Details on the mass balances are listed in in the supplemental information, including the nonzero mole fractions in each stream.

4.3.2 Energy calculations

4.3.2.1 Electrolyzer Electrolysis energy demands are determined by using the cell voltage E_{cell} and current i_{total} to calculate the cell power $P_{electrolysis}$. Energy is normalized per mole of product ($W_{electrolysis}$):

$$P_{electrolysis} = E_{cell} \cdot i_{total} \tag{30}$$

$$W_{electrolysis} = \frac{P_{electrolysis}}{\dot{N}_{product}} \tag{31}$$

4.3.2.2 Separation units Gases are separated by pressure-swing adsorption. They are modeled to be 100% selective to a single gas; their real selectivity is >95% for relevant cases.[77] Oxalic acid is separated from the catholyte by gas-antisolvent precipitation at the base case. We model it to be 100% selective. The ideal work of separation of a binary mixture for an isothermal and isobaric separation process is adjusted by the second-law efficiency to determine the separation energy. This is more accurate for the PSA units than for GASP. Efficiency for the GASP process should be higher since it is a nearly thermodynamic process and energy requirements for pressurization and stirring are typically

low.[42]

$$W_{sep(j)}^{ideal} = R \cdot T \cdot \left(\sum_i x_i \cdot \ln x_i \right) \cdot \frac{\dot{N}_{\text{total (j)}}}{\dot{N}_{\text{product}}} \tag{32}$$

$$= R \cdot T \cdot (x_i \cdot \ln x_i + (1 - x_i) \cdot \ln (1 - x_i)) \cdot \frac{\dot{N}_{\text{total (j)}}}{\dot{N}_{\text{product}}} \tag{33}$$

$$W_{sep(j)}^{real} = \frac{W_{sep(j)}^{ideal}}{\zeta} \tag{34}$$

where $W_{sep(j)}^{ideal}$ and $W_{sep(j)}^{real}$ are the ideal and real work to separate stream j per mole of product, R is the gas constant (8.314 J/mol·K), T_{sep} is the separation temperature (313 K), x is the mole fraction of one of the binary components as determined from a mole balance, and ζ is the second-law separation efficiency. These energies are reported per mole of CO_2R product. At the base case, we assume that ζ_{PSA}= 7% and ζ_{GASP} = 20%. Although energy efficiencies are not reported for antisolvent crystallization in the literature, this is a typical efficiency for a pressurized separation with the addition of phases, such as absorption and stripping.[78]

We also estimate energy for drying the catholyte. Desiccant systems for liquid dehydration operate through a two-cycle process – adsorption of water by a dessicant, and reactivation by stripping water from the dessicant. Adsorption of water is carried out by passing the liquid inlet stream through a packed column of granular desiccant. Regeneration is carried out by hot compressed air passed through the column. To operate continuously, two towers are used so that adsorption can continue while one bed is being regenerated. Energy is mainly used to compress air to regenerate the dessicant bed when it is fully saturated. We assume that the pump is 70% efficient.[79] The volume of compressed air is based on an empirical estimation for dessicant drying. The pump delivers 20% of the inlet stream volume at 100 psig (689,475 Pa).[80,81] We assume a residence time of 10 minutes for liquid in the bed.

$$P_{drier} = \frac{\Delta P \dot{V}}{\zeta_{pump}} = 0.2\dot{V}_{(24)} \cdot \frac{6.894 \times 10^5 \text{ Pa} - 1 \times 10^5 \text{ Pa}}{0.7} \tag{35}$$

Here, P_{drier} is the power of the compression pump in W, ΔP is the pressure change through the pump, ζ_{pump} is the efficiency of the pump, and $0.2\dot{V}_{(24)}$ is the volumetric flow rate of the purge gas for regeneration.

We neglect energy demands for deionization, gas drying, and pressure changes. Temperature is assumed to be maintained at 40 °C by heat integration only.

4.4 Capital and operating cost estimation

4.4.1 Capex

Capex (capital cost) is calculated for each process unit. Bare module costs (C_{BM}) describe the purchase and installation of equipment. This includes process equipment which is customized, like pressure vessels, and off-the-shelf process machinery, like pumps. We adjust reference equipment costs for inflation using the Chemical Engineering Plant Cost Index (CEPCI) for 2024. The battery limits ("on-site") units include electrolysis, balance-of-plant and separations only. This means that feedstocks (CO_2, DI water) and utilities (electricity) come from external vendors and are only costed as operating expenses (Table 3). Solvent and supporting electrolyte costs are both operating and capital costs – capital costs to supply the initial the process volume, and operating costs for solvent makeup and supporting electrolyte replacement. The non-aqueous supporting electrolyte in particular is completely recycled until its replacement. The electrolyzer cost is based on manufacturing analysis by Badgett et al.,[45] with linear scaling. Since our electrolyzer model is based on the use of an expensive iridium catalyst for the OER, we use their stack cost for a PEM electrolyzer, which also includes an iridium anode. Lowering iridium loadings or finding alternative OER catalysts in acid would reduce this capital cost. Another possible change could arise from different gas diffusion layer costs, since the material must prevent non-aqueous flooding rather than aqueous flooding. Hofsommer et al.[82] have achieved this using solid polymer GDEs, and Konig et al. through carbon-free GDEs[83], which have negligible costs compared to the catalysts. The electrolyzer cost at the base case is \$5,174/m^2 (CEPCI 2024), assuming an intermediate manufacturing rate (some economy of scale in CO_2R deployment).[45] Although Badgett et al. calculate electrolyzer cost to formate, the cathode catalyst cost is a small contributor, allowing the use of this capex for other aqueous and non-aqueous products as well. This is comparable to the capex calculated by Shin et al. (\$4300/m^2 (CEPCI 2020)).[38] The balance of plant, including compression and pumping capital costs, is 35% of the electrolyzer bare module cost, based on the H2A model for PEM water electrolysis.[84,85] Pressure-swing adsorbers were priced based on a reference cost of \$3.5 million (CEPCI 2024) for a 1000 m^3/hr capacity with a scaling factor of 0.7. Gas-antisolvent precipitation costs are based on previous estimates of €0.95 million (CEPCI 2004) for a process that uses 2,160 kg of CO_2.[57,58] We assume that this process uses just enough CO_2 to exceed its solubility limit at 10 bar. Therefore, the amount of CO_2 used depends on its solubility in the solvent at 10 bar, calculated by Henry's law in Workbook S1. Sensitivity to the cost of liquid-liquid separation does not rely on the scaling from GASP, instead scaling the capex relative to the cost of separating a 1,000 mol/hr inlet stream into the GASP unit, i.e. $C_{BM,\text{ L/L}} = C_{BM,\text{ L/L, reference}} \cdot (\frac{\dot{N}_{\text{total (22)}}}{1000 \text{ mol/hr}})^{0.7}$. The corresponding capex for GASP at a 1000 mol/hr inlet at the base case is $C_{BM,\text{ L/L, reference}} = \$37,950$.

While aqueous CO_2R uses pH-neutral potassium bicarbonate as a solvent, non-aqueous CO_2R occurs with an acidic anolyte (and can make oxalic acid). We therefore cost stainless steel units throughout the separations for the non-aqueous case, which includes a material factor of 1.3.[86] We neglect the cost of spares, storage and surge tanks, initial catalyst charges, controls, and computers.

Total direct permanent investment includes any cost of additional facilities constructed, which is typically zero in this model as we use retail electricity prices and ambient conditions for feedstocks. If desired, utility-scale batteries can be modeled using Code S1. We ignore the cost of site preparation, service facili-

ties, utility plants, and auxiliary facilities like steam or electric generation. The total depreciable capital includes all capital costs for the actual installed equipment. This includes contractors and contingencies, which we cost as 18% of the direct permanent investment, broken down into 3% for contractors and 15% for contingencies. This is very low for contingency for a new technology; typically 35 – 100% is estimated for a novel process. Land, patent royalties and plant startup costs are ignored. If land is purchased, its cost is usually recovered at the end of the plant life; however, we assume a coarse estimate for renting land and buildings in the opex calculations instead, especially given the small process scale (Table 3). The total permanent investment includes all capital investments except working capital. In this work, we refer to "capex" as the total permanent investment. Working capital covers operating costs before the plant begins to sell product, such as inventory, accounts receivable, raw materials, other operational requirements. It is typical to coarsely estimate working capital as 15 – 25% of the total depreciable capital. The total capital cost including working capital is the total capital investment.

Pressure changers (pumps, compressors) are typically inexpensive and are not made to order. Rather than explicitly costing them here, we include their costs in the balance of plant. Hydrogen separation is easy since its kinetic diameter is much smaller than CO, CO_2, or ethylene, allowing the use of size-selective zeolite beds in pressure-swing adsorption. Although separating CO from CO_2 is more challenging, proprietary units in industry rely on modified adsorbents.[87]

Table 2 Capital cost breakdown

Cost	Formula	Source
Bare module cost of equipment, C_{BM}		
Electrolyzer	\$5,714/m^2, 1.12× installation factor, CEPCI 2024: $\frac{800}{773.1} \cdot \frac{\$5,000}{\text{m}^2} \cdot A \cdot 1.12$	45
Solvent	Total volume is 2× drier volume: Solvent cost per kg $\cdot \rho_{solvent} \cdot 2 \cdot \dot{V}_{(24)} \cdot 10$ minutes	Workbook S1
Supporting electrolyte	Total volume is 2× drier volume: $\frac{\$10}{kg_{\text{NR}_4\text{X}}} \cdot MW_{\text{NR}_4\text{X}} \cdot c_{supporting} \cdot 2 \cdot \dot{V}_{(24)} \cdot 10$ minutes	63
Catholyte drier	2 pressure vessels, 10 minute residence time + initial dessicant material $2 \cdot 1.3 \cdot \frac{800}{509.7}\left(\$5000 + \$1400 \cdot (\dot{V}_{(24)} \cdot 10 \text{ minutes})^{0.7}\right) + 2 \cdot \frac{\$8}{kg_{MS4A}} \cdot 700\frac{kg_{MS4A}}{m^3} \cdot \dot{V}_{(24)} \cdot 10$ minutes	51
Balance of plant	$34.5\% \cdot C_{BM,\text{ electrolyzer}}$	84
Cathode PSA1 – CO_2 vs products	Stainless steel, CEPCI 2024 $1.3 \cdot \frac{800}{596.2} \cdot \$1,989,043 \cdot \left(\frac{\dot{V}_{(13)}}{1000\text{m}^3/\text{hr}}\right)^{0.7}$	38
Cathode PSA2 – gas products vs H_2	Stainless steel, CEPCI 2024 $1.3 \cdot \frac{800}{596.2} \cdot \$1,989,043 \cdot \left(\frac{\dot{V}_{(15)}}{1000\text{m}^3/\text{hr}}\right)^{0.7}$	38
Anode PSA3 – CO_2 vs O_2 (aqueous only)	Stainless steel, CEPCI 2024 $1.3 \cdot \frac{800}{596.2} \cdot \$1,989,043 \cdot \left(\frac{\dot{V}_{(7)}}{1000\text{m}^3/\text{hr}}\right)^{0.7}$	38
GASP	$1.3 \cdot \frac{800}{444.2} \cdot \frac{\$1.24}{€} \cdot €950,000 \cdot \left(\frac{\dot{N}_{\text{total (22)}} x_{solvent\,(22)} \cdot \text{CO}_2 \text{ solubility in solvent}}{2160 \text{ kg}_{\text{CO2}}/\text{hr}}\right)^{0.7}$	57,58
Total capital cost		
Total bare-module investment, C_{TBM} or inside battery limits capital cost, C_{ISBL}	$\sum_{units} C_{BM}$	
Total of direct permanent investment, C_{DPI}	$C_{TBM} + C_{alloc}$; $C_{alloc} = 0$ in most cases	86
Contractor and contingency cost, C_{cont}	3% for contractors, 15% for contingencies $18\% \cdot C_{DPI}$	86,88
Total depreciable capital, C_{TDC}	$C_{DPI} + C_{cont}$	86
Total permanent investment, C_{TPI}	$C_{TDC} + 0$	86
Working capital, C_{WC}	15%, recovered at end of plant lifetime $15\% \cdot C_{TDC}$	86
Total capital investment, C_{TCI}	$C_{WC} + C_{TPI}$	86

4.4.2 Opex

Opex is costed as feedstocks, utilities, operations, maintenance, overheads, taxes and insurance, and general expenses. We model these according to standard process design guidelines, not accounting for any differences that may arise for electrochemical processes, like overheads scaling by area or unit number rather than volume. We base operating costs on the methods of Sinnott et al.[51]

Feedstocks are based on a CO_2 capture cost per ton and the costs of deionized water and solvent. Utilities are calculated from the total energy consumed by the electrolyzer and separation units, all of which is assumed to be electricity with no heating or cooling duties. The maintenance cost is 4% of the capital cost apart from the electrolyzer. The stack replacement cost is the direct permanent investment cost of the electrolyzer, and the material replacement cost is the cost of the dessicant medium, which is replaced every 2 years,[89] as well as the supporting electrolyte replaced every 5 years. Although there are two dessicant beds, only one is operated at a given time while the other is regenerated, so the cost of dessicant replacement every 2 years is the volume of one bed only. The initial loading of dessicant, electrolyzer stack, and supporting electrolyte are costed as capex. To normalize to an annual cost, the cost of all replacements over the plant lifetime is divided by the plant lifetime in years. A stack lifetime of 1 year is chosen as the baseline, based on a small fraction of the lifetime estimates for water electrolyzers. PEM water electrolyzers, which use a similar zero-gap design with precious metal catalysts, have a lifetime today of 20,000 – 60,000 hours.[90] Since CO_2R is a less developed technology, an intermediate lifetime of 8,500 hours (1 year) was chosen. No additional cost of non-aqueous supporting electrolyte is included as a feedstock, since we assume that it is stable for 5 years and can be recycled fully without any salt accumulation. The dominance of utility costs for electrochemical processes stands out in comparison to most petrochemical processes, where feedstock costs dominate. Total sales are based on the following market prices: \$2/kg_{H_2}, \$0.85/kg_{CO}, \$0.7/$kg_{\text{oxalic acid}}$ (North America), and \$0.96/kg_{ethylene}.

Table 3 Operating expense breakdown

Cost ($/yr)	Formula	Source
Feedstocks		
Captured CO_2	CO_2 capture cost per kg $\cdot \dot{M}_{\text{CO}_2\text{ fresh feed (1)}} \cdot 365 \cdot CF$	91
Deionized water	DI water cost per kg $\cdot \dot{M}_{\text{water, fresh feed (10)}} \cdot 365 \cdot CF$	92
Solvent	Solvent cost per kg $\cdot \dot{M}_{\text{solvent, fresh feed (18)}} \cdot 365 \cdot CF$	Workbook S1
Utilities		
Electricity	$U_{product} \cdot$ Electricity cost ($/kWh) $\cdot \dot{M}_{\text{product}} \cdot 365 \cdot CF$	
Operations		
Operating labor, 4 shifts for continuous fluids process	$4 \cdot \frac{\$80,000}{\text{year}}$	51,93
Supervision	25%· Operating labor	51
Direct labor and supervision	50%· Operating labor and supervision	51
Maintenance		
Stack replacement, per year	$\texttt{round}\left(\frac{\text{Plant lifetime}}{\text{Stack lifetime}}\right) \cdot C_{BM,\text{electrolyzer}} \cdot \frac{1}{\text{Plant lifetime}}$	
Dessicant replacement, per year	$\texttt{round}\left(\frac{\text{Plant lifetime}}{2\text{ years}}\right) \cdot \frac{\$8}{kg_{\text{MS4A}}} \cdot 700\frac{kg_{\text{MS4A}}}{m^3} \cdot \dot{V}_{(24)} \cdot 10\text{ minutes}$	
Supporting electrolyte replacement, per year	$\texttt{round}\left(\frac{\text{Plant lifetime}}{5\text{ years}}\right) \cdot C_{BM,\text{supporting}}$	
Maintenance, per year	$4\% \cdot (C_{TBM} - C_{BM,\text{electrolyzer}})$	51
Overhead		
Operating overhead	65%· Labor, supervision and maintenance	86
Property and taxes		
Property taxes and insurance, per year	$2\% \cdot C_{TBM}$	51
Environmental charges, per year	$1\% \cdot C_{TBM}$	51
Land rent, per year	$2\% \cdot C_{TBM}$	51
General expenses		
Selling (or transfer) expense	1%· Sales (of CO_2R product and H_2)	86
Direct research	4.8%· Sales	86
Allocated research	0.5%· Sales	86
Administrative expense	2%· Sales	86
Management incentive compensation	1.25%· Sales	86

5 Data availability

The data supporting this article have been included as part of the Supplementary Information:

- Supplementary Information. Detailed mass balance calculations, Figures S1 – S14, and Tables S1 – S7.
- Workbook S1. Excel file containing parameters for techno-economic assessment of non-aqueous CO_2R.
- Workbook S2. Excel file containing literature review data corresponding to Figure 1 and Figure S1.
- Code S1. Compressed folder (.zip) containing code to model electrolyzer, perform mass and energy balances, model techno-economics, and generate figures.

6 Author contributions

S.C.D. developed the concept, built the model, and wrote the article. J.R. guided the work. All authors contributed to the discussion, review, and editing of the manuscript.

7 Conflicts of interest

There are no conflicts to declare.

8 Acknowledgements

The authors thank Jon-Marc McGregor and Hussain Almajed for useful discussions. The authors gratefully acknowledge the support for this work provided by the National Science Foundation through the NSF CAREER Award (Award Number 2340693) and the Welch Foundation under grant number F-2076.

References

1 J. Resasco and A. T. Bell, *Trends in Chemistry*, 2020, **2**, 825–836.

2 M. J. Orella, S. M. Brown, M. E. Leonard, Y. Román-Leshkov and F. R. Brushett, *Energy Technology*, 2020, **8**, 1900994.

3 S. C. Da Cunha and J. Resasco, *Nature Communications*, 2023, **14**, 5513.

4 S. A. Hawks, V. M. Ehlinger, T. Moore, E. B. Duoss, V. A. Beck, A. Z. Weber and S. E. Baker, *ACS Energy Letters*, 2022, **7**, 2685–2693.

5 J. A. Rabinowitz and M. W. Kanan, *Nature Communications*, 2020, **11**, 5231.

6 P. De Luna, C. Hahn, D. Higgins, S. A. Jaffer, T. F. Jaramillo and E. H. Sargent, *Science*, 2019, **364**, eaav3506.

7 Z. Huang, R. G. Grim, J. A. Schaidle and L. Tao, *Energy & Environmental Science*, 2021, **14**, 3664–3678.

8 S. C. Da Cunha and J. Resasco, *ACS Energy Letters*, 2024, **9**, 5550–5561.

9 J. Vos, A. Ramírez and M. Pérez-Fortes, *Renewable and Sustainable Energy Reviews*, 2025, **213**, 115454.

10 Y. Tomita, S. Teruya, O. Koga and Y. Hori, *Journal of The Electrochemical Society*, 2000, **147**, 4164.

11 A. Kusoglu and A. Z. Weber, *Chemical Reviews*, 2017, **117**, 987–1104.

12 S. Ma, R. Luo, J. I. Gold, A. Z. Yu, B. Kim and P. J. A. Kenis, *Journal of Materials Chemistry A*, 2016, **4**, 8573–8578.

13 Y. Hori, *Modern Aspects of Electrochemistry*, Springer New York, New York, NY, 2008, vol. 42, pp. 89–189.

14 M. Gautam, F. Nkurunziza, M. C. Mulvehill, S. S. Uttarwar, D. T. Hofsommer, C. A. Grapperhaus and J. M. Spurgeon, *ChemSusChem*, 2024, **17**, e202301337.

15 D. T. Hofsommer, M. Gautam, S. S. Uttarwar, C. A. Grapperhaus and J. M. Spurgeon, *ACS Applied Energy Materials*, 2023, **6**, 2624–2632.

16 M. Gautam, D. T. Hofsommer, S. S. Uttarwar, N. Theaker, W. F. Paxton, C. A. Grapperhaus and J. M. Spurgeon, *Chem Catalysis*, 2022, **2**, 2364–2378.

17 D. T. Hofsommer, Y. Liang, S. S. Uttarwar, M. Gautam, S. Pishgar, S. Gulati, C. A. Grapperhaus and J. M. Spurgeon, *ChemSusChem*, 2022, **15**, e202102289.

18 *Fundamentals and Applications of Organic Electrochemistry*, ed. T. Fuchigami, S. Inagi and M. Atobe, Wiley, 1st edn, 2014.

19 K. Izutsu, *Electrochemistry in Nonaqueous Solutions*, Wiley, 1st edn, 2009.

20 A. M. Haregewoin, A. S. Wotango and B.-J. Hwang, *Energy & Environmental Science*, 2016, **9**, 1955–1988.

21 R. J. Gomes, R. Kumar, H. Fejzić, B. Sarkar, I. Roy and C. V. Amanchukwu, *Nature Catalysis*, 2024, **7**, 689–701.

22 J.-M. McGregor, J. T. Bender, A. S. Petersen, L. Cañada, J. Rossmeisl, J. F. Brennecke and J. Resasco, *Nature Catalysis*, 2025, **8**, 79–91.

23 I. Bagemihl, L. Cammann, M. Pérez-Fortes, V. Van Steijn and J. R. Van Ommen, *ACS Sustainable Chemistry & Engineering*, 2023, **11**, 10130–10141.

24 M. König, S.-H. Lin, J. Vaes, D. Pant and E. Klemm, *Faraday Discussions*, 2021, **230**, 360–374.

25 S. S. Uttarwar, D. T. Hofsommer, C. Hartman, F. Nkurunziza, M. Gautam, W. F. Paxton, C. A. Grapperhaus and J. M. Spurgeon, *ACS Sustainable Chemistry & Engineering*, 2024, **12**, 13263–13273.

26 M. Jouny, G. S. Hutchings and F. Jiao, *Nature Catalysis*, 2019, **2**, 1062–1070.

27 J. B. Greenblatt, D. J. Miller, J. W. Ager, F. A. Houle and I. D. Sharp, *Joule*, 2018, **2**, 381–420.

28 V. Boor, J. E. B. M. Frijns, E. Perez-Gallent, E. Giling, A. T. Laitinen, E. L. V. Goetheer, L. J. P. Van Den Broeke, R. Kortlever, W. De Jong, O. A. Moultos, T. J. H. Vlugt and M. Ramdin, *Industrial & Engineering Chemistry Research*, 2022, **61**, 14837–14846.

29 J. M. Spurgeon and B. Kumar, *Energy & Environmental Science*, 2018, **11**, 1536–1551.

30 *Oxalic Acid Price Index*, `https://businessanalytiq.com/procurementanalytics/index/oxalic-acid-price-index/`.

31 A. N. Amenaghawon, J. E. Ayere, U. O. Amune, I. C. Otuya, E. C. Abuga, C. L. Anyalewechi, O. V. Okoro, J. A. Okolie, P. K. Oyefolu, S. O. Eshiemogie, B. E. Osahon, M. Omede, S. A. Eshiemogie, S. Igemhokhai, M. O. Okedi, H. S. Kusuma, O. E. Muojama, A. Shavandi and H. Darmokoesoemo, *Environmental Research*, 2024, **251**, 118703.

32 K. Kharas, *Sustainable production of oxalic acid, ethylene glycol, ethylene, propylene and oxygen by electrolytic reaction of carbon dioxide with water*, 2014, `https://patentimages.storage.googleapis.com/3e/03/61/9e41cdd1d4a65f/WO2014065839A1.pdf`.

33 *Oxalic Acid Market Analysis*, 2023, `https://www.chemanalyst.com/industry-report/oxalic-acid-market-2969`.

34 *Oxalic Acid Market Size, Share, and Trends 2024 to 2034*, 2024, `https://www.precedenceresearch.com/oxalic-acid-market`.

35 M. A. Murcia Valderrama, R.-J. Van Putten and G.-J. M. Gruter, *European Polymer Journal*, 2019, **119**, 445–468.

36 S. Ikeda, T. Takagi and K. Ito, *Bulletin of the Chemical Society of Japan*, 1987, **60**, 2517–2522.

37 E. L. Clark and A. T. Bell, *Energy and Environment Series*, Royal Society of Chemistry, Cambridge, 2020, pp. 98–150.

38 H. Shin, K. U. Hansen and F. Jiao, *Nature Sustainability*, 2021, **4**, 911–919.

39 M. H. Barecka, J. W. Ager and A. A. Lapkin, *iScience*, 2021, **24**, 102514.

40 B. S. Crandall, B. H. Ko, S. Overa, L. Cherniack, A. Lee, I. Minnie and F. Jiao, *Nature Chemical Engineering*, 2024, **1**, 421–429.

41 D. M. Ruthven, S. Farooq and K. S. Knaebel, *Pressure Swing Adsorption*, VCH Publishers, Inc., 1994.

42 A. Weber, R. Kümmel and T. Kraska, *Supercritical Fluids as Solvents and Reaction Media*, Elsevier, 2004, pp. 429–448.

43 J. Jung and M. Perrut, *The Journal of Supercritical Fluids*, 2001, **20**, 179–219.

44 R. I. Masel, Z. Liu, H. Yang, J. J. Kaczur, D. Carrillo, S. Ren, D. Salvatore and C. P. Berlinguette, *Nature Nanotechnology*, 2021, **16**, 118–128.

45 A. Badgett, M. Ruth, A. Crow, G. Grim, Y. Chen, L. Hu, L. Tao, W. Smith, K. Neyerlin and R. Cortright, *Journal of Cleaner Production*, 2022, **351**, 131564.

46 E. A. Dos Reis, G. T. S. T. Da Silva, E. I. Santiago and C. Ribeiro, *Energy Technology*, 2023, **11**, 2201367.

47 D. Wakerley, S. Lamaison, J. Wicks, A. Clemens, J. Feaster, D. Corral, S. A. Jaffer, A. Sarkar, M. Fontecave, E. B. Duoss, S. Baker, E. H. Sargent, T. F. Jaramillo and C. Hahn, *Nature Energy*, 2022, **7**, 130–143.

48 J. Fischer, T. Lehmann and E. Heitz, *Journal of Applied Electrochemistry*, 1981, **11**, 743–750.

49 *Oxaquim will invest seven million euros in the expansion of the Alcañiz plant*, 2024, https://oxaquim.com/oxaquim-will-invest-seven-million-euros-in-the-expansion-of-the-alcaniz-plant/.

50 L. D. Schmidt, *The engineering of chemical reactions*, Oxford Univ. Press, New York, NY, 2nd edn, 2005.

51 R. Sinnott and G. Towler, *Chemical Engineering Design*, Elsevier, 5th edn, 2009.

52 R. Wang, S. Yuan, R. Xue, M. Cheng, X. Yan, S. Shen, Y. Guo and J. Zhang, *Energy & Fuels*, 2025, **39**, 3942–3953.

53 C. BalReddy, S. Ram, A. Kumar, R. Bharti and P. Das, *Chemistry – A European Journal*, 2019, **25**, 4067–4071.

54 S. Ram, P. Mehara, A. Kumar, A. K. Sharma, A. S. Chauhan, A. Kumar and P. Das, *Molecular Catalysis*, 2022, **530**, 112606.

55 B. A. Olsen, *Journal of Chromatography A*, 2001, **913**, 113–122.

56 L. J. Crossey, *Geochimica et Cosmochimica Acta*, 1991, **55**, 1515–1527.

57 M. Rantakylä, *Doctor of Technology*, Helsinki University of Technology, Espoo, Finland, 2004.

58 J. Clavier, W. Majewski and M. Perrut, *Process Technology Proceedings*, Elsevier, 1996, vol. 12, pp. 639–644.

59 J. Shi, F.-x. Shen, F. Shi, N. Song, Y.-J. Jia, Y.-Q. Hu, Q.-Y. Li, J.-x. Liu, T.-Y. Chen and Y.-N. Dai, *Electrochimica Acta*, 2017, **240**, 114–121.

60 A. Diaz-Duque, A. P. Sandoval-Rojas, A. F. Molina-Osorio, J. M. Feliu and M. F. Suarez-Herrera, *Electrochemistry Communications*, 2015, **61**, 74–77.

61 W. Riemenschneider and M. Tanifuji, *Ullmann's Encyclopedia of Industrial Chemistry*, Wiley, 1st edn, 2011.

62 *Market size of ethylene worldwide in 2021, with a forecast until 2030*, 2022, https://www.statista.com/statistics/1349781/ethylene-global-market-size/.

63 L. Chen, M. Sharifzadeh, N. Mac Dowell, T. Welton, N. Shah and J. P. Hallett, *Green Chem.*, 2014, **16**, 3098–3106.

64 M. Ue, K. Ida and S. Mori, *Journal of The Electrochemical Society*, 1994, **141**, 2989–2996.

65 J. Spurgeon, *Electrochemical Reduction of Flue Gas Carbon Dioxide to Commercially Viable C2-C4 Products (Final Report)*, DOE-UofL–0031916, 1972205, 2023.

66 M. Jouny, W. Luc and F. Jiao, *Industrial & Engineering Chemistry Research*, 2018, **57**, 2165–2177.

67 S. Dongare, M. Zeeshan, A. S. Aydogdu, R. Dikki, S. F. Kurtoğlu-Öztulum, O. K. Coskun, M. Muñoz, A. Banerjee, M. Gautam, R. D. Ross, J. S. Stanley, R. S. Brower, B. Mucharla, R. L. Sacci, J. M. Velázquez, B. Kumar, J. Y. Yang, C. Hahn, S. Keskin, C. G. Morales-Guio, A. Uzun, J. M. Spurgeon and B. Gurkan, *Chemical Society Reviews*, 2024, **53**, 8563–8631.

68 M. König, J. Vaes, E. Klemm and D. Pant, *iScience*, 2019, **19**, 135–160.

69 G. Bilicic and S. Scroggins, *Lazard's Levelized Cost of Energy Analysis — Version 16.0*, 2023.

70 D. T. Whipple, E. C. Finke and P. J. A. Kenis, *Electrochemical and Solid-State Letters*, 2010, **13**, B109.

71 Y. Xu, R. K. Miao, J. P. Edwards, S. Liu, C. P. O'Brien, C. M. Gabardo, M. Fan, J. E. Huang, A. Robb, E. H. Sargent and D. Sinton, *Joule*, 2022, **6**, 1333–1343.

72 C. Amatore and J. M. Saveant, *Journal of the American Chemical Society*, 1981, **103**, 5021–5023.

73 O. K. Coskun, Z. Bagbudar, V. Khokhar, S. Dongare, R. E. Warburton and B. Gurkan, *Journal of the American Chemical Society*, 2024, **146**, 23775–23785.

74 M. T. Koper, *Journal of Electroanalytical Chemistry*, 2011, **660**, 254–260.

75 R. Kas, A. G. Star, K. Yang, T. Van Cleve, K. C. Neyerlin and W. A. Smith, *ACS Sustainable Chemistry & Engineering*, 2021, **9**, 1286–1296.

76 L.-C. Weng, A. T. Bell and A. Z. Weber, *Energy & Environmental Science*, 2019, **12**, 1950–1968.

77 X. Ma, J. Albertsma, D. Gabriels, R. Horst, S. Polat, C. Snoeks, F. Kapteijn, H. B. Eral, D. A. Vermaas, B. Mei, S. De Beer and M. A. Van Der Veen, *Chemical Society Reviews*, 2023, **52**, 3741–3777.

78 T. Moore, D. I. Oyarzun, W. Li, T. Y. Lin, M. Goldman, A. A. Wong, S. A. Jaffer, A. Sarkar, S. E. Baker, E. B. Duoss and C. Hahn, *Joule*, 2023, **7**, 782–796.

79 *Fundamentals of momentum, heat, and mass transfer*, ed. J. R. Welty, Wiley, Danver, MA, 5th edn, 2008.

80 R. Marshall, *Desiccant Dryers – Ten Lessons Learned*, Compressed air best practices technical report, 2014.

81 *What Are Dual Tower Regenerative Desiccant Air Dryers?*, 2023, https://www.vmacair.com/blog/dual-tower-regenerative-desiccant-air-dryers-work.

82 D. T. Hofsommer, I. R. Zamborini, S. S. Uttarwar, C. A. Phipps, M. Gautam, F. Nkurunziza, C. A. Grapperhaus and J. M. Spurgeon, *ACS Sustainable Chemistry & Engineering*, 2024, **12**, 882–892.

83 Y. Alvarez-Gallego, X. Dominguez-Benetton, D. Pant, L. Diels, K. Vanbroekhoven, I. Genné and P. Vermeiren, *Electrochimica Acta*, 2012, **82**, 415–426.

84 *Hydrogen Analysis Production Models (H2A v3.2018)*.

85 David Peterson, James Vickers and Dan DeSantis, *Hydrogen*

Production Cost from PEM Electrolysis - 2019, 19009, 2020.

86 W. D. Seider, D. R. Lewin, J. D. Seader, S. Widagdo, R. Gani and K. M. Ng, *Product and process design principles: synthesis, analysis and evaluation*, Wiley, New York, Fourth edition edn, 2017.

87 *Industrial Gases in Petrochemical Processing: Chemical Industries*, ed. H. H. Gunardson, CRC Press, 0th edn, 1997.

88 *Perry's chemical engineers' handbook*, ed. D. W. Green and M. Z. Southard, McGraw Hill Education, New York, Ninth edition, 85th anniversary edition edn, 2019.

89 H. M. Malino, *A Short Cut Method for Evaluating Molecular Sieve Performance*, 2019.

90 O. Schmidt, A. Gambhir, I. Staffell, A. Hawkes, J. Nelson and S. Few, *International Journal of Hydrogen Energy*, 2017, **42**, 30470–30492.

91 A. Baylin-Stern and N. Berghout, *Is carbon capture too expensive?*, International energy agency technical report, 2021.

92 T. Alerte, A. Gaona, J. P. Edwards, C. M. Gabardo, C. P. O'Brien, J. Wicks, L. Bonnenfant, A. S. Rasouli, D. Young, J. Abed, L. Kershaw, Y. C. Xiao, A. Sarkar, S. A. Jaffer, M. W. Schreiber, D. Sinton, H. L. MacLean and E. H. Sargent, *ACS Sustainable Chemistry & Engineering*, 2023, **11**, 15651–15662.

93 *Occupational Employment and Wages, May 2023: 51-8091 Chemical Plant and System Operators*.